


FABIO MATERA

DESIGN AND TESTING OF A PASSIVE MONOPOLAR DMFC STACK FOR PORTABLE POWER APPLICATIONS

SUPERVISORE:	PROF. L. FORTUNA	- DIEES
TUTOR:	PROF. A. FICHERA	- DIIM
CORRELATORI:	DR. A. ARICÒ	– ITAE-CNR
	DR. V. BAGLIO	– ITAE-CNR

Summary

Purpose of this work

This work is the Ph.D. thesis developed at the Faculty of Engineering – Department of Electrical, Electronic and System Engineering (DIEES) at the University of Catania for the XXIII Ph.D. Course held under the supervision of Prof. L. Fortuna and coordinated by Prof. A. Fichera (DIIM - Department of Industrial and Energy Engineering).

The purpose of this work is to develop a portable Direct Methanol Fuel Cell power supply designed to operate in passive mode. This job makes a step forward over the research already started at the CNR-ITAE in 2007 by the group lead by Dr. A. Aricò and whom I am a Staff member.

Acknowledgments

This work is the result of many efforts made by very different people which I would like to express my gratitude here. First of all, the colleagues (which I first consider friends) of the CNR-ITAEt their spontaneous and precious scientific contribution in the experimental part of this work. The research here discussed, and specifically the DMFC experimental results, starts from the experiments performed by the research team lead by Dr. A. Aricò and whom I am a member as a researcher together with Dr. V. Baglio, Dr. A. Stassi, Dr. A Di Blasi and the leader, Dr. A. Aricò. Their contribution has been decisive in all the development of this work. I wish to acknowledge the whole group for their support and the great job done. We must also acknowledge the financial support from “Regione Piemonte” (Italy) through the Micro Cell project (Delibera della Giunta Regionale no. 25-14654 del 31/01/05) which represented the first base from which this research has started.

My appreciation goes to Dr. Giusy La Rocca (Politecnico of Torino, Italy) for her contribution and to the friends and colleagues of the Faculty of Engineering, University of Catania, for their precious expertise.

Last but not least, my gratitude goes to my dear friends Eddie and Daniela Rojas (Jacksonville, FL), for their patience and hints which made this work complete.

1. Introduction to fuel cells

1.1. Definition of Fuel Cell

A Fuel Cell (which acronym is FC) is a power generator able to directly convert the chemical energy "stored" in a fuel into electric energy by means of a chemical reaction. The simplest and most known scheme of Fuel Cell is shown in Fig. 1.1, which relates to a widely known system defined "Polymer Electrolyte Fuel Cell (PEFC)". Its main components are:

1. the anode electrode, where negative ions are produced from the fuel, which in this case is Hydrogen;
2. the cathode electrode, where positive ions migrates from the anode through the electrolyte;
3. an electrolyte, interposed between anode and cathode which acts as ion carrier from anode to cathode (acid electrolyte, like in a PEFC) or cathode to anode (alkaline electrolyte) and, at the same time, acts as a physical barrier between the fuel and the oxidant;
4. the MEA, which is the assembly of the two electrodes (anode and cathode) and the membrane in between;

5. the plates, which have channels for fuel and oxidant, and act as current collectors and electrical connections. The terminal plates, which are the most external, usually incorporate the connectors for inlet and outlet of fuel and oxidant; the intermediate plates connect two adjacent cells and have channels on both sides (one side for the anode, one side for the cathode). This is the reason why they are also named bipolar plates;
6. a peripheral sealing all around the MEA, to seal the cells and avoid fuel loss;
7. an hardware, which includes current collectors, gas inlet and outlet connectors, bolts and other parts needed to keep all the cells stacked into a whole "package" named simply "fuel cell stack".

1.2. Basic fuel cell electrochemistry and thermodynamics

In a fuel cell, or more specifically in a PEFC, the fuel, i.e. hydrogen, is decomposed at the anode into its electron and its proton (or positive ion H^+). the principle of operation is described by the following reactions [1]:

- Anode reaction: $H_2 \rightarrow 2H^+ + 2e^-$

- Cathode reaction: $\frac{1}{2} O_2 + 2H^+ + 2e^- \rightarrow H_2O$
- Overall reaction: $H_2 + \frac{1}{2} O_2 \rightarrow H_2O$ (liquid) + 286 kJ/mol (at 25°C)

At the anode, the H^+ ions migrate through the electrolyte (see Fig. 1.1), to the cathode. Electrons flow (which is by definition a current) to the cathode through the external circuit, which is the load. Theoretically, in a perfectly reversible conversion, the product of the reaction is electric power and pure water. In the real world all the energy transformations are irreversible and not all the energy can be converted into useful electricity and some is converted (not necessarily wasted) into heat, depending on the operating conditions. The equation which describes the energy conversion in a fuel cell is the Gibbs expression:

$$\Delta G = \Delta H - T\Delta S \qquad [1.1]$$

where ΔG is the total energy change of reactants (named also Gibb's Free Energy) given by the variation of enthalpy ΔH and the variation of entropy $T\Delta S$. The entropy variation represents hence the loss of energy from its theoretical maximum value given by the enthalpy change. The values of ΔG, ΔH and ΔS are usually tabulated as function of temperature.

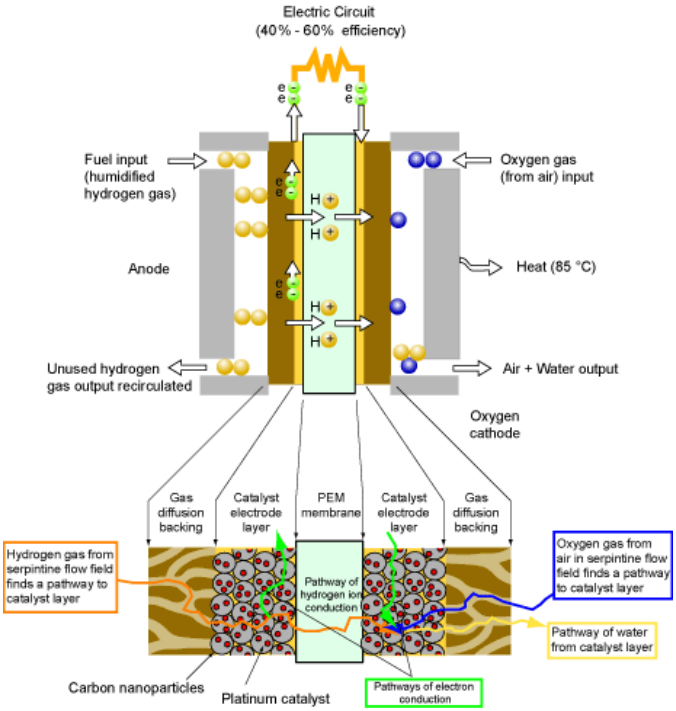

Fig. 1.1: scheme of a fuel cell. (Source: Neutron Imaging Facility, NIST - National Institute of Standards and Technology, USA)

The efficiency can hence be expressed as the ratio between the real output and the theoretical output at fixed conditions:

$$\eta = \Delta G / \Delta H \qquad [1.2]$$

or, by substituting eq. [1.1] in eq. [1.2]:

$$\eta = 1 - (T\Delta S / \Delta H) \qquad [1.3]$$

It is evident that:

- the term $T\Delta S$ represents the loss of efficiency;
- an increase of temperature T represents a loss in terms of efficiency. This aspect is actually true only in principle, as an increase in temperature increases also the reaction performance, by easing the reactants to combine, and decreases the sensitivity of catalyst to some poisonous compounds, i.e. the effect of carbon monoxide over Platinum. The final result is that an increase in temperature, within the strength limits of the materials, results in better overall performances. Hence it follows that the common tendency is to increase the operating temperature of the stack in most fuel cell application.

The typical behavior (or more exactly the “polarization plot”) of a fuel cell is the V-I plot, which describes the variation of the output voltage as a function of output current.

Polarization plot

The polarization plot describes how the fuel cell voltage varies with the output current. An example is shown in Fig. 1.2. The polarization (or V-I) curve of a fuel cell can be subdivided into three main regions, each with its own behavior. The first region is called the **activation** region. It features a rapid decrease of voltage due to the energy gap needed to activate the chemical reaction. The second region, also called **polarization** or **Ohmic** region, features an almost linear decrease of voltage with the output current, due to Ohmic resistance of the system. The last region is the **diffusion** region, where chemical reactants face increasing diffusion problems flowing through the MEA, resulting in a rapid drop of voltage down to zero due to a lack of reactants.

Fuel cell background and status

Fuel cells are not a modern discovery. Their invention goes back to 1839, by Sir William Grove, a lawyer and scientist. They have been further developed by Sir Francis T. Bacon, during 1920's, who demonstrated the first hydrogen-oxygen 5 kW fuel cell stack in August 1952. Lately, in the same year,

Allis-Chalmers demonstrated a 15 kW system, able to power a tractor, based on the same Bacon's concept but operating at lower pressure and temperature. Except these demonstration prototypes, a practical application of this technology started only in the early 1960's with the Gemini space program led by NASA (Fig. 1.3).

In Gemini V there were used the first polymer-based fuel cells (PEFC), produced by General Electric, which doubled the permanence record established by Gemini IV thanks to the superior performances of fuel cells over batteries. Lately, the PEFC systems were substituted by Alkaline Fuel Cells (AFC) developed by Pratt & Whitney Aircraft. Starting from late 80's to nowadays, fuel cells have been identified as one of the most promising power sources for the next future in most applications where power can be supplied in form of electrical energy. This is due to their relative simple concept, the high efficiency and the great flexibility of their design. From a market perspective, in most cases fuel cells compete with very well established technologies and in saturated markets, hence they need to outperform the status in term of performance, which has been already achieved, and cost, which instead is still a hard target to reach. Anyway, fuel cells systems have been demonstrated to be reliable and performing in any field, overcoming in some cases the status where cost has a less importance over performance, such as in submarines, portable military equipment and spacecrafts.

The “fuel cell” definition covers a wide group of different power systems (Table 1.1) [2], each with its own typical features in terms of materials, performances, range of application and fuel used. The application of each technology depends mostly on which aspect (i.e. operating temperature,

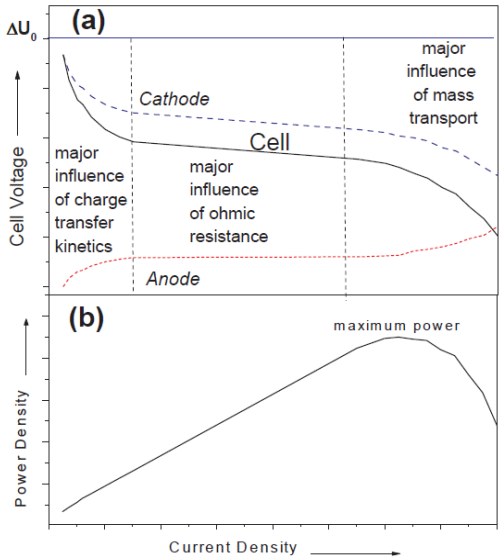

Fig. 1.2: typical polarization plot of a fuel cell [1.13]. The upper chart shows the change of voltage vs. current. The lower chart is the output power vs. current derived from the expression P = V I

fuel and electricity-to-heat power rate) is preferred as well as cost targets.

1.3. Fuel Cell applications

It has been already mentioned that fuel cells are power generators which can be used anywhere power can be supplied as electric power. Their size can easily fit any application, from the smallest to the largest, being the economical convenience and the benefits achievable compared to a conventional solution, the only limit to their application. Actually they have been applied in many different fields: from space to

	AFC (Alkaline)	PEMFC (Polymer Electrolyte Membrane)	DMFC (Direct Methanol)	PAFC (Phosphoric Acid)	MCFC (Molten Carbonate)	SOFC (Solid Oxide)
Operating temp. (°C)	<100	60–120	60–120	160–220	600–800	800–1000 low temperature (500–600) possible
Anode reaction	$H_2 + 2OH^- \rightarrow 2H_2O + 2e^-$	$H_2 \rightarrow 2H^+ + 2e^-$	$CH_3OH + H_2O \rightarrow CO_2 + 6H^+ + 6e^-$	$H_2 \rightarrow 2H^+ + 2e^-$	$H_2 + CO_3^{2-} \rightarrow H_2O + CO_2 + 2e^-$	$H_2 + O^{2-} \rightarrow H_2O + 2e^-$
Cathode reaction	$\frac{1}{2}O_2 + H_2O + 2e^- \rightarrow 2OH^-$	$\frac{1}{2}O_2 + 2H^+ + 2e^- \rightarrow H_2O$	$3/2\,O_2 + 6H^+ + 6e^- \rightarrow 3H_2O$	$\frac{1}{2}O_2 + 2H^+ + 2e^- \rightarrow H_2O$	$\frac{1}{2}O_2 + CO_2 + 2e^- \rightarrow CO_3^{2-}$	$\frac{1}{2}O_2 + 2e^- \rightarrow O^{2-}$
Applications	Transportation Space Military Energy storage systems			Combined heat and power for decentralised stationary power systems	Combined heat and power for stationary decentralised systems and for transportation (trains, boats, ...)	
Realised Power	Small plants 5–150kW modular	Small plants 5–250 kW modular	Small plants 5 kW	Small – medium sized plants 50kW – 11MW	Small power plants 100-kW- 2 MW	Small power plants 100–250kW
Charge Carrier in the Electrolyte	OH^-	H^+	H^+	H^+	CO_3^{2-}	O^{2-}

Table 1.1: different fuel cell technologies and features.

telecommunication, from automotive to small power supply devices. In the following there are some of the most representative examples of fuel cell systems for the following applications:

- Aerospace ;
- Submarine ;
- Aviation ;
- Automotive ;
- Stationary power and distributed generation;
- UPS, Backup and other small size portable power systems.

Portable applications, which are the subject of this work, will be explained more in detail in Chapter 2.

Space applications

The space race in 1950 and 1960 promoted the development of fuel cells. In search of an improved energy source for on-board electricity, NASA chose fuel cells to power space missions and funded over 200 research projects awarded to industry and universities. General Electric developer the first polymer electrolyte membrane fuel cell (PEFC or PEMFC) for Gemini space missions. The first mission using fuel cells was Gemini

V, in 1965, which doubled the space flight record of Gemini IV mission thanks to the fuel cell system, which outperformed the battery used on previous missions. In '70s NASA Space Center equipped Apollo, Apollo-Soyuz, SpaceLab and Space Shuttle (including the movie-star Apollo 13 space module) with an Alkaline Fuel Cell module (see Fig. 1.3). This system was intended to supply electrical power to the equipment and potable water (which is produced by the fuel cell as result of the energy conversion) to the crew.

Even nowadays, with the Space Shuttle ships, there are still AFC power modules, demonstrating the high reliability of these systems.

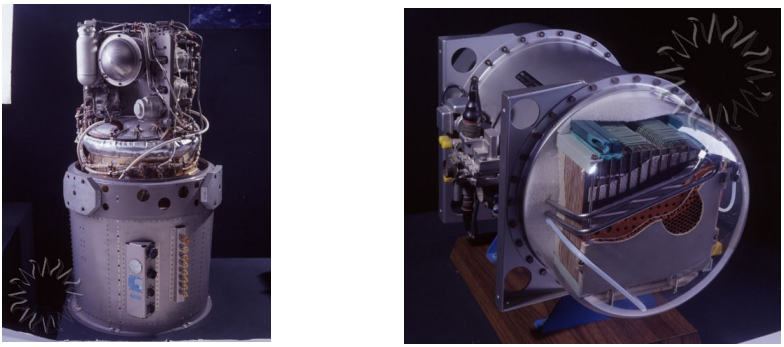

Fig. 1.3: Alkaline Fuel Cell module used in Apollo 13 (left) and Polymer Electrolyte Fuel cell module used in Gemini (right) (source: NASA)

Submarine applications

In submarines, fuel cells are used as main AIP (Air Independent Propulsion) systems for underwater operation in place of the batteries. The use of fuel cells has increased the underwater operational time from the original 5 days (using a closed-loop diesel engine and battery pack) to more than 3 weeks (with H_2 / O_2 PEFC) (see Fig. 1.4), operating without any exhaust heat, thermal trace, noiseless and hence virtually undetectable. Nowadays most of the actual submarines are designed with fuel cell based AIP.

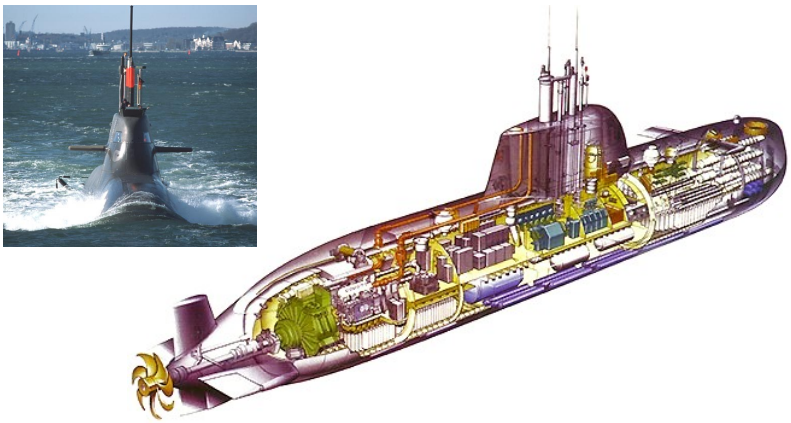

Fig. 1.4: Class 214 submarine (Howaldtswerft Deutsche Werft - HDW) picture in operation (up left) and a cross section scheme (right). source: Naval Technology

Aviation applications

A very interesting fuel cell technology, named “regenerative fuel cells” has been used in a specialty airplane (see Fig. 1.5). These systems are able to operate in a reversible two ways:

- as a power generator, by converting hydrogen and oxygen into electricity, heat and water,
- as a water electrolyzer, by separating water into hydrogen and oxygen using electricity as energy source.

Such system was used in the unmanned Helios aircraft, designed to operate uninterruptedly at very high altitudes. The airplane was equipped with photovoltaic panels, distributed over the upper face of the wings (which span was over 75 m), and regenerative fuel cell systems. During daytime, solar radiation was converted into electricity by photovoltaic panels, which provided power to the propeller electric motors and, eventually, the excess energy to the regenerative fuel cell system. This latter operated as electrolyzer, splitting water into hydrogen and oxygen. During nighttime flights, the regenerative fuel cells operated as power generators, powering the propellers by converting the stored hydrogen and oxygen into electricity.

Beside such innovative solutions, a more conventional system has been used to power the Boeing's fuel cell aircraft, showed in Fig. 1.6. It still represent the first example of manned airplane powered by a fuel cell system tested in real

Fig. 1.5: Helios aircraft (NASA) powered by a regenerative fuel cell system and photovoltaic modules. (Source: NASA Archive Website)

Fig. 1.6: Boeing's fuel cell aircraft, one of the first examples of manned fuel cell aircraft.

environment, showing the technical feasibility of such systems for aviation purpose.

Automotive applications

In automotive applications, fuel cells have shown a great potential as an alternative solution for electric vehicles. Using hydrogen as fuel, they have no local emissions (the only emission is pure water and heat) and hydrogen can be produced from renewable energy by means of electrolysis. On ground vehicles there have been tested also other fuel cell technologies than hydrogen: after the early prototypes, equipped with a AFC, which required high grade purity hydrogen and oxygen, there have been used also SOFC (by Delphi, USA) and DMFC (Daimler, FIAT and others). None of these systems have reached a satisfactory performance over the PEFC technology, mainly due to a complicate system management (especially for AFC and SOFC systems) and a very high cost due to very high catalyst load for DMFC. PEFC systems are instead actually tested [3] and widely used as the only viable alternative to conventional internal combustion (or IC) engines.

One of the most complete DMFC powered car which has run a complete set of on-road tests has been the NECAR 5, a Mercedes-Benz A-Class sedan car powered by a DMFC stack fed with liquid methanol (see Fig. 1.7).

Another fuel cell ground application is forklift. Forklift propulsion systems and distributed power generation are identified as potential fuel cell applications for near-term markets. These systems are widely used to move heavy loads both at indoor and outdoor locations. Hence there is a strong interest in use a non polluting fast rechargeable system which meets both indoor (operated by battery systems) and outdoor (operated by IC systems) requirement as well as a high autonomy, comparable with that of IC conventional systems [4].

Fig. 1.7: the Daimler's NECAR 5 A-Class sedan, featuring a DMFC engine fueled with liquid methanol. (Source: Daimler Web Site)

Stationary power and distributed generation.

The lower range kW-size power generators can feed a single home as well as being connected to a local grid or the electric network. Yet without taking into account hydrogen production and supply, which must be considered into a complete and realistic scenario, these devices represent the first step over a "distributed generation" of stationary power generation. A widely distributed network of such systems, with local generation of main power from renewable energy sources and hydrogen used as an energy storage fuel, represents the concept of future energy generation. Fuel cells are very suitable also as stand-alone stationary power generators, especially where premium power (or peak) is needed without any compromise with pollutant emissions. In this case fuel cell systems may have some CHP (Combined Heat and Power) capability, although usually there is a PEFC stack operating at around 80°C. For such a case, the fuel may vary from hydrogen to natural gas. If natural gas is used, it is processed separately in a fuel processor to obtain an hydrogen-rich gas [5], containing a very little level of CO (less than 100 ppm or even lower). Actually some of these systems are already available on the market, although the energy cost is still very high.

A widely used system, as example, is produced by UTC Power (a unit of Universal Technologies Corporation). These systems, operating with a PAFC (Phosphoric Acid Fuel Cell), integrate in its shelter all the core systems (see Fig. 1.8):

1. the fuel processor, to convert natural gas to an hydrogen-rich gas. This system includes these subsystems:

   - the hydro-desulfurization unit, which removes the sulfur compounds which might be present in the fuel as odorizer.
   - the steam reforming unit, which converts methane into an hydrogen-rich gas following the reaction:

     $2CH_4 + 3H_2O = 7H_2 + CO + CO_2$

   - the integrated low-temperature Shift converter, which converts the poisoning CO into hydrogen and carbon dioxide given the reaction:

     $CO + H_2O = H_2 + CO_2$

   - an ammonia scrubber, to remove the ammonia at the anode generated by the conversion of methane because of the presence of nitrogen.
   - a condenser, to recover the water vapor at the exhaust of the system and reuse it for the steam reforming and shift reactions.

2. the PAFC system, which provides also heat together with electricity (CHP mode). The overall efficiency in CHP mode can be up to 90% and the nominal electric efficiency up to 40%. The lifetime is 10 years.

3. the power converter to connect the system to the electric grid.

Other systems have been proposed and tested in real conditions [6, 7] to show the potential of such technology and study the performances in real applications.

Fig. 1.8: PureCell stationary fuel cell power system, by UTC Fuel Cells. The system has been installed in several locations worldwide. It can provide electric power as well as heat with very low emissions and high performances. Legenda: (1) Fuel Processor. (2) Fuel Cell stacks. (3) Power conditioner. (Source: www.utcfuelcells.com)

UPS, Backup and other small size portable power systems

Fuel cells are the only available choice when it is needed a portable systems in the range of 0,5-1 kW which can be operated indoor, in presence of people without polluting or emitting unacceptable levels of noise (Fig. 1.9 and 1.10). This is the case of large, modular backup systems for data storage centers, as well as small UPS systems [6] that can be kept and operated indoor even at home, just beside the desk or the PC console. An example is shown in Fig. 1.9, with two Ballard's AirGen 1,2 kW UPS systems operating within an office environment, without harnessing human health or comfort.

Fig. 1.9: Ballard's Airgen power systems. The rated power of each system is 1,2 kW and the system is already available on the consumer market.

Meanwhile most of these systems are already available on the market, hydrogen is not yet available on the retail market. Hence most of these application, and in general the future of hydrogen fuel cell technology, is mostly conditioned by the safety regulations and permissions which can allow or block the use of hydrogen as a fuel for domestic [8] or automotive appliances.

Hydrogen is not the only renewable fuel considered for portable fuel cells actually. Direct methanol fuel cells for portable devices are widely proposed and investigated as a very promising technology in the short term [9]. Methanol is a renewable energy carrier as it can be produced from waste biomass by mean of specific chemical processes. In Fig. 1.10 there is a Smart Fuel Cell SFC A25 power system. It is a DMFC system - sold by Smart Fuel Cell – which is intended to be used in a range of applications, including recreational vehicles and sailing boats. To cover the energy demand of four entire days only one fuel cartridge of about 2 kg is required. A comparable energy content of lead-acid batteries weighs about 100 kg. In addition it is being marketed as a remote industrial power source for traffic and telecommunication systems, danger warning and weather stations. It also recharges batteries, wherever it might be required.

Fig. 1.10: Smart Fuel Cell power system. On the left, the refilling tank with methanol.

1.4. References

1. L. Carrette1+, K. A. Friedrich1 and U. Stimming, Fuel Cells - Fundamentals and Applications, Fuel Cells, 2001, 1, 1, 5-39

2. Frano Barbir, PEM Fuel Cells - Theory and Practice, Elsevier, 2005. ISBN 0-12-078142-5

3. N. Rajalakshmi, S. Pandian, K.S. Dhathathreyan, Vibration tests on a PEM fuel cell stack usable in transportation application, International Journal of Hydrogen Energy, Volume 34, Issue 9, May 2009, Pages 3833-3837, ISSN 0360-3199, DOI: 10.1016/j.ijhydene.2009.03.002.

4. Amgad Elgowainy, Linda Gaines, Michael Wang, Fuel-cycle analysis of early market applications of fuel cells: Forklift propulsion systems and distributed power generation, International Journal of Hydrogen Energy, Volume 34, Issue 9, May 2009, Pages 3557-3570, ISSN 0360-3199, DOI: 10.1016/j.ijhydene.2009.02.075.

5. Liangliang Sun, Yuqiang Liu, Wei Wang, Ran Ran, Yan Huang, Zongping Shao, Methane catalytic decomposition integrated with on-line Pd membrane hydrogen separation for fuel cell application, International Journal of Hydrogen Energy, Volume 35, Issue 7, 2008 International Hydrogen Forum (HyForum2008), 2008 International Hydrogen, April 2010, Pages 2958-2963, ISSN 0360-3199, DOI: 10.1016/j.ijhydene.2009.05.069.

6. Ferraro Marco, Sergi Francesco, Cretì Pasquale, Dispenza Giorgio, Matera Fabio, Sapienza Cristoforo, Andaloro Laura and Antonucci Vincenzo, Evaluation of an UPS system based on Direct Hydrogen PEM Fuel Cell, WHEC 16, Lyon France, 13 - 16 June 2006

7. Muhsin Tunay Gencoglu, Zehra Ural, Design of a PEM fuel cell system for residential application, International Journal of Hydrogen Energy, Volume 34, Issue 12, UGHEK 2008, UGHEK 2008, June 2009, Pages 5242-5248, ISSN 0360-3199, DOI: 10.1016/j.ijhydene.2008.09.038.

8. S. Brennan, A. Bengaouer, M. Carcassi, G. Cerchiara, G. Evans, A. Friedrich, O. Gentilhomme, W. Houf, A. Kotchourko, N. Kotchourko, S. Kudriakov, D. Makarov, V. Molkov, E. Papanikolaou, C. Pitre, M. Royle, R. Schefer, G. Stern, A.G. Venetsanos, A. Veser, D. Willoughby, J. Yanez, Hydrogen and fuel cell stationary applications: Key findings of modelling and experimental work in the HYPER project, International Journal of Hydrogen Energy, In Press, Corrected Proof, Available online 11 June 2010, ISSN 0360-3199, DOI: 10.1016/j.ijhydene.2010.04.127.

9. S.K. Kamarudin, F. Achmad, W.R.W. Daud, Overview on the application of direct methanol fuel cell (DMFC) for portable electronic devices, International Journal of Hydrogen Energy, Volume 34, Issue 16, 4th Dubrovnik Conference, 4th Dubrovnik Conference, August 2009, Pages 6902-6916, ISSN 0360-3199, DOI: 10.1016/j.ijhydene.2009.06.013.

10. Energy, U.S.D., Fuel cell handbook. In5th ed. ed., Science Applications International Corporation E&G Services Parson Inc, 2000.

11. Cook B. An introduction to fuel cell technology. J Mater Sci, 2001; R33:109–34.

12. Wee JH., Review - Which type of fuel cell is more competitive for portable application: direct methanol fuel cells or direct borohydride fuel cells. J Power Sources 2006; 161:1–10.

2. Portable fuel cells

2.1. Introduction

Since portable electronic devices have been spread on the mass market, their performances have steadily increased together with their power consumption. Larger screens and advanced features, such as integrated GPS, wireless network connectivity and mobile phone, have increased the power consumption, reducing the autonomy. Hence, autonomy has become one of the crucial issues for such systems, despite actual advanced batteries [1] have reduced the recharge time to 2-4 hours as well as increased the energy density [2] and further developments are expected in the next future. Today the average autonomy of a modern hand-held system is usually shorter than 4 hours under intensive use and there is always the need to plug the device to the electric network or a car. From such situation there is a strong interest on more advanced and performing power devices which could conveniently improve the autonomy of portable electronics [3]. This need for extended power and the attracting consumer market business have pushed many companies in developing different solutions of which fuel cells are, in perspective, the most promising [4-5].

2.2. Methanol as a fuel

Although hydrogen is the most used fuel for fuel cell application, actually it is a quite complicate fuel to manage for small portable devices such as hand-held devices. Metal hydride hydrogen tanks are usually heavy, although quite safe. Moreover hydrogen fuel, needed to refill the tank, is not on the consumer market and worldwide most regulations still consider it a dangerous explosive industrial product rather than a commercial fuel. Hence actually hydrogen is not a very suitable as a fuel for hand-held devices.

In any power application, the choice of a fuel must deal with many constraints: market acceptance, consumers attitude, safety regulations and so on. On a practical side, consumers are not accustomed to gaseous fuels, meanwhile they're used to liquid fuels such as those used in gas lighters. On the safety side, an hydrogen leakage would be hardly perceived by a customer, meanwhile a methanol leakage would be easily sensed as any liquid spill. Methanol is easy to be brought to the consumer market, easy to handle and to store for long periods. This is one of the reason why it is considered an interesting option from portable devices stakeholders and most of worldwide battery manufactures [5-10].

Methanol is known as methyl alcohol or wood alcohol. It occurs naturally in the environment, being generated by biological processes occurring in vegetation, microorganisms and other living species. It is water soluble and is

biodegradable in either the presence or the absence of air. It does not generate any significant odor. Described by the chemical formula CH_3OH, methanol is a colorless liquid which has already a number of industrial and consumer market uses. As a basic building block for hundreds of chemical products, methanol is being used safely and effectively for everything from plastics and paints to construction materials and windshield washer fluid. Liquid methanol contains more energy per unit weight than any stored form of hydrogen applicable for man portable power applications. It is significantly safer to handle than any form of stored hydrogen of significant energy content. Like other alcohols, methanol is flammable; however, small volumes of methanol packaged in sealed plastic containers present little, if any, danger to potential users in portable power applications. Approved fuel cartridges may be locally produced or transported anywhere in the world via air-freight, making methanol the ideal fuel choice for portable fuel cells.

Meanwhile fuel cell systems may virtually operate with any of the available fuel cell technologies, PEFC, using hydrogen, and DAFC, using methanol and ethanol, are the most suitable for small and portable devices. The choice between these two systems is mostly related to whether a more complex fuel system or a more expensive fuel cell system is preferred. Meanwhile a PEFC system, operating with dry hydrogen and ambient air, needs an accurate water management and a more expensive and complicate fuel system, due to the presence of gaseous hydrogen as fuel, usually DAFC have not such

complication because the fuel is a liquid mix between water and alcohol. At system level, usually both the systems are designed to operate in dead-end mode at the anode, but for DAFC there is the need to vent the CO_2 produced from the oxidation of the fuel (Fig. 2.1). The use of a DAFC instead needs an higher catalyst load (usually an order of magnitude higher than PEFC running on pure hydrogen fuel) and a different membrane able to reduce cross-over issues. Hence, DAFC, compared to PEFC, face a significantly lower

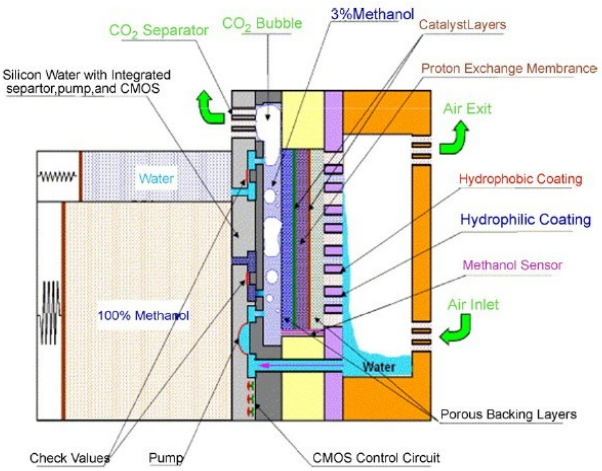

Fig. 2.1: a complete scheme of DMFC system, as proposed by [11].

performance (efficiency, power density, etc.) and an higher cost due to the massive use of expensive catalysts.

In portable systems, both PEFC and DAFC systems are usually designed to operate at the cathode with ambient air at ambient pressure and temperature, hence it is important to properly design the cathode to ensure a correct and efficient air circulation. Two solutions may be applied: forced ventilation, by means of a small blower, and natural convective ventilation, by leaving the cathode exposed to ambient air and let the differential pressure replenish the depleted oxygen. At the cathode there is also the need to remove the by-product of the reaction, pure water, which is slightly more for a DAFC due to the cross-over from the anode side through the membrane. This water might be, more or less conveniently, recovered to replenish the water at the anode which migrated to the cathode through the membrane. The presence of a liquid fuel has some advantage over a gaseous fuel. First, there is no need for humidification, which is a key issue for PEFC. Second, fuel handling is simpler, as well as refueling the system. Hence methanol is a preferred solution for most of the portable fuel cell power devices.

2.3. Status of development of portable DMFC systems

Portable DMFC are in competition with batteries as portable power sources. A comparison [2.12] has shown the potential of

such systems as portable power generator in military application (Fig. 2.2). Recently, some FC based systems have been proposed on the prototype market to power portable devices, in the range 1 – 30 W of rated power. From the early systems (H-Power) designed to power portable radio for military use, a range of fully integrated power systems have been developed for applications such as Auxiliary Power Units (APU) or battery extender. All these use PEFC technology in its two variations, direct hydrogen and direct methanol. If a direct hydrogen system is preferred, the fuel is gaseous hydrogen stored in a metal hydride alloy within a cylindrical tank. These fuel storage systems are quite expensive, heavy and their storage capability is usually small. Also refueling the tank is relatively complex because it has to be refueled from an external source at higher pressure and hydrogen is not available on the consumer market. Despite this feature, they are a relatively safe storage system due to low pressure and their robust yet simple design.

Where a direct methanol system is preferred, then methanol is stored in a tank operating at ambient pressure, close to the FC system or also integrated within the same FC stack. Methanol handling, as a liquid fuel, is very simple, although yet toxic. As a fuel, it is relatively easy to be found on the retail market; it is a by-product of most of distillery processes or as a natural product of vegetable decomposition from fermentation; furthermore it doesn't harms the environment. When dealing with a liquid, it is important to note that the fuel tank is sensible to the orientation of the system, as well as to shocks,

shaking and roll-overs. Hence, the tank and the system must be operated in the proper position to avoid fuel spill and feed issues.

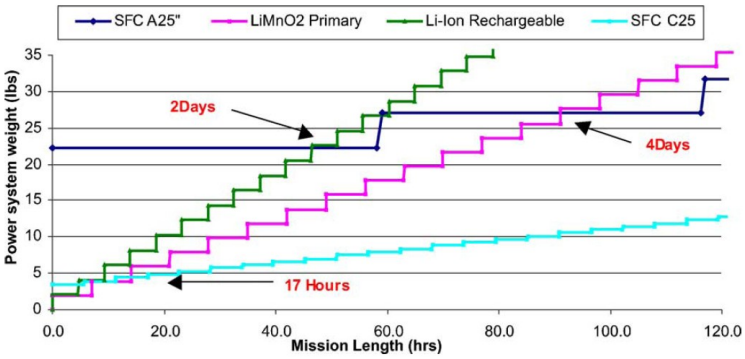

Fig. 2.2: Smart Fuel Cell A25 and C25 vs. battery power; weight comparison for 25W continuous load profile [2.12]

2.4. Research activity on portable DMFC systems

Fuel cells for portable applications are still in a stage between base research and early market prototypes. This is due to the great attraction coming from the consumer market of portable devices and the strong need of further improvements on most of the components of a DMFC. At research level, there is a great interest over the enhancements of each single component of the fuel cell, as well as the problems related to DMFC technology are distributed over most of its parts (membrane, catalyst, electrodes, etc.).

Electrolyte

At component level, several aspects are challenging the researchers on portable DMFC systems. At electrolyte (or membrane**)** level, it can be said that the conventionally used poly-sulphon based membranes (Du-Pont's Nafion® and similar) face an excessive permeability (crossover) to methanol. It brings to two main problems: a loss of efficiency (for the loss of useful fuel) and a loss of voltage (also said mixed potential), as the presence of the fuel at the anode decreases the voltage across the two electrodes. A conventional solution, which can reduce crossover, is the use of a thicker membrane, but this also increases the electrical resistance of

the MEA, with worsen overall electrical performances of the system.

A different approach is develop an electrolyte based basically on a modified polymer over the existing membrane (usually Nafion based) by adding different polymers (i.e. SPEEKK) [13] or by adding other compounds to Nafion (i.e. silica micro-particles, ceramic binders) [14]. In both cases these solutions give better or comparable performances than Nafion, also in terms of mechanical properties at high temperatures (over 80°C), such as water uptake, reduced swelling, higher tensile strength. Research is also focused in developing new polymers [15-18].

Beside reducing fuel crossover, some of these solutions usually feature better performances in ion conductivity than Nafion, but such better performance are achieved in a tighter temperature range than Nafion. Outside the optimum range, performances usually significantly worsen, hence the substitution of Nafion electrolyte depends mostly on the operating conditions. In some case, better performances are counterbalanced from a sensibly reduced lifetime of the membrane, which increases the cost of the system.

It must also mentioned than cationic conductive polymer are not the only choice for DMFC. Similarly to AFC, anionic conductive electrolyte have been developed and tested [19] with interesting results.

Catalyst

The catalyst is the true component, together with the electrolyte, which makes fuel cell operation possible. Hence a large number of researches are focused in developing improved catalysts for methanol oxidation. One of the most sensible issue of catalyst is its cost, as it is usually derived from noble metals alloy such as Platinum, Ruthenium and other very expensive noble metals. Furthermore, the methanol oxidation requires very high catalyst loading, increasing significantly the cost of DMFC systems. This issue can be addressed by researching a different yet cheaper catalyst with comparable activity or by reducing the catalyst loading yet offering a comparable activity. In fact not all the catalyst is effectively used at the catalytic layer as some is not reached by the reactants. Hence a good practice is find an electrode structure able to maximize the catalyst availability yet reducing the overall loading [20]. Other techniques are focused on manufacture the two substrate catalytic layer (diffusive and properly said catalytic layer) with a one-step process, trying to reduce manufacture cost and time of catalyst deposition. [21].

MEA assembly

The MEA (Membrane and Electrode Assembly) is the core component of a fuel cell, being the remaining component considered as “hardware”. It is made by three main components: the anode, the solid electrolyte membrane and the

cathode. The MEA is hence a three layer component which are assembled in a whole by hot pressing or simply kept tight together by the plates assembly. Both anode and cathode electrodes are often manufactured into three layers: from the outer to the inner, there is the substrate, which acts as a support and ensures the electric continuity between the catalytic sites and the bipolar plates; the diffusive layer, which has the property to let the reactant diffuse homogeneously to the inner substrate while keeping the electrical contact for ion charges; the catalytic layer, which is in direct contact with the electrolyte, which is the effective site of reaction and where ions species are produced. Of course all these layers are a continuum.

One of the main problem of MEA is its durability under stressing conditions. If one of the three components looses the contact with the others, the performances decrease rapidly as well as it may result in a reduced electrical contact. This effect is generally studied at single component (electrode and electrolyte) level as well as at whole MEA level. The components, as well as the whole MEA, are tested in extreme conditions, such as high voltage and humid operation, high temperature or combined effect of temperature, voltage and humidity conditions. The most common problems are related to carbon support corrosion (high voltage and humidity conditions), membrane mechanical instability or rupture (high temperature), disassembly of the MEA components (high temperature and pressure or mechanical stress), catalyst microstructure degradation [22].

2.5. System Design

Research is dedicated also in developing new designs for the plates, designing new flowfields which might better fit the needs of the system. In some cases there have been studied some fancy designs, as those derived from fractal theory [23]. At system level, the research is mainly focused in designing a system which integrates in a single or a very few components many of the subsystems, including power conversion devices, pumps and valves. Under this aspect, there are two main philosophies: one is mostly based on MEMS architectures and microfluidic systems, which are derived mostly from silicon-based microchip industry and practices (Fig.s 2.3-2.4) [24-26].

Micro-DMFC systems from MEMS technology

Successful application of MEMS technology, which is traditionally used in the semiconductor industry, in various systems such as internal sensors, biomedical and optical systems, has made it a promising candidate for the miniaturization of fuel cell system, especially PEMFC and DMFC. Several works have been conducted to investigate the feasibility of MEMS technology in micro-DMFC system. This technology provides a possibility of economical future mass production and has the potential to solve problems which are critical in the conventional stack technology such as the fabrication of micro-porous membranes optimized for two

phase transport, the plasma polymerization of ion conducting polymers and the fabrication of transport optimized micro-flow fields with varying dimensions [27]. MEMS technology can control the fine and precise flows of the fuel, air and water in the electrodes, which may improve the current and power densities in a small fuel cell [28]. The prospective potential of MEMS technology for miniaturization of fuel cell system has stimulated interests from researchers and industries. Apart from the drastically decreased size, the application of MEMS technology in a fuel cell production usually results in the change of cell materials, such as the silicon wafer, instead of the conventional graphite, for bipolar plates. In fact, the major advantage of MEMS technology is in making the bipolar plate smaller and with higher precision, coupled with the potential of mass production.

The use of silicon wafer in micro-fuel cells enables more variation in MEA fabrication. The silicon material system also encompasses a range of materials used in the semiconductor integrated circuit industry such as silicon oxides, nitrides and carbides as well as metals like aluminum and titanium [29].

Nafion membranes are inadequate to standard micro-fabrication techniques, i.e. they cannot be easily patterned with standard photo-lithography and their volumetric variations due to hydration are a real problem for the assembly with silicon substrates [30-31]. Regardless of the MEA used in cell system, the common fabrication processes in MEMS technology are more or less the same. Firstly, micro-fluid channels and feed

holes are inscribed onto the wafer by applying various etching methods, such as deep reactive ion etching (DRIE) with a negative photo resist that acts as an etching mask, or wet chemical etching. Then a layer of Au or Cu/Au is sputtered on silicon wafer as the current collector, with titanium/tungsten layer as adhesive. There are two options for the application of catalysts, either to coat the catalyst on the electrodes and hot-press it with the membrane or to coat it directly onto the surface of the silicon substrates. Current approaches for MEMS assembly are using single or double Si wafers for substrates and a combination of novel materials. The design of the micro-DMFC and its working principle are depicted in Fig. 2.3 [24]. The fuel solution ($CH_3OH/H_2SO_4/H_2O$) is fed to the anode side of the unit cell where the catalyst promotes the CH_3OH to release electrons, carbon dioxide, and protons.

The electrons travel in the form of an electric current that can be utilized before it returns to the cathode side of the fuel cell where the oxidant solution (O_2-sat./H_2SO_4/H_2O) has been fed. On the other hand, molecular oxygen reacts at the cathode with proton being transported through the membrane from the anode and produces water, thereby completing the oxidation–reduction process. The anode to cathode contact is the thickness of the Nafion (50μm) as illustrated in Fig. 2.5. Here, the path length from anode to cathode is the clearance between the two microchannels, which is 100μm. Connecting both the anode and the cathode to an external load makes it possible to produce electric power. The approach shown in Fig. 2.3 has

several advantages and differs in many ways from previous designs:

- It is of planar structure and essentially an unfolded fuel cell as shown in Fig. 2.3, which integrates the anode and cathode onto a single Si surface. Whereas, the bi-layer design uses separate Si wafers with channels for the anode and cathode.

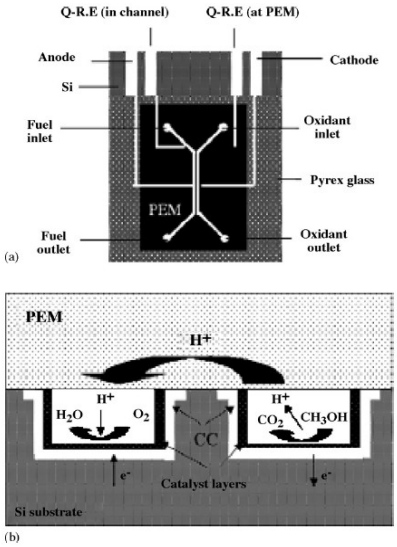

Fig. 2.3: principle of operation of a micro-DMFC derived from MEMS technology. [24]

- The fuel and oxidant are supplied to the cell in isolated, separate micro-channels. Both the fuel and oxidant are distributed in micro-channels throughout the wafer, and they both possess an exhaust. The isolation of fuel and oxidant precludes one from crossing the fuel and oxidants streams.

- The characteristic length of the system that is the distance that the protons must travel from anode to cathode is very short. This makes the system less sensitive to ohmic impedance effect.

- The efficiency of the current collectors is high, because the catalyst layers are supported on the metal directly. In addition, the current collectors are directly deposited in the microchannels. The current does not need to be pulled out by relatively large metal lines.

- Catalyst electrodes are directly fabricated in the bottom and sidewalls of the micro-channels.

In Fig. 2.4 there is a scheme of the fabrication process of a micro-DMFC chip using typical MEMS processing [24]. In Fig. 2.5 there is a different fuel cell structure, named micro - DEFC* (Direct Ethanol Fuel Cell), where ethanol is used

* It is of a common use the acronym "DAFC" to include all the alcohol fueled fuel cells, such as methanol and ethanol.

instead on methanol (which is highly toxic) for medical applications [25].

A different approach is that derived from the conventional design of DMFC by using simple and very basic systems with reduced size of components. Most of these systems operate in air-breathing passive mode, hence without pumps, blowers,

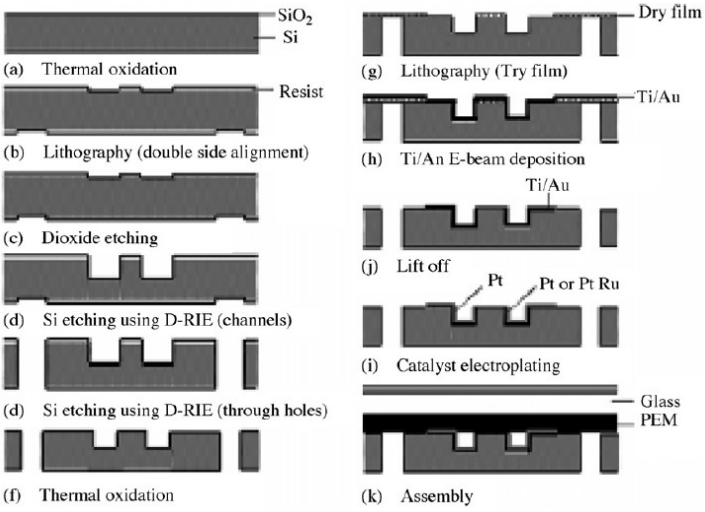

Fig. 2.4: schematic of fabrication of a micro-DMFC chip [24-25]

heaters and any other passive auxiliary loads. These are the probably most simple concept of DMFC.

These systems have been designed in several different schemes, from the simplest single cell, shown in Fig. 2.6 and Fig. 2.7, to the more complex stacked – planar mixed schemes shown in Fig. 2.8. The planar configuration features each single cell of the system positioned side-by-side, as shown in Fig. 2.8 under the "banded" definition. In this case the contact between the single cells is obtained through a thin metallic film which connects one cathode to the anode of the adjacent cell.

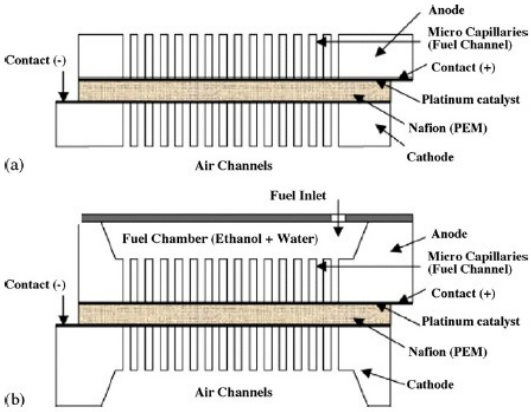

Fig. 2.5: micro-DEFC using ethanol instead of methanol (which is highly toxic) for medical applications [25].

Some examples of such technique are shown in Fig. 2.6 [32], 2.8 [33], 2.7 [34]. Other configurations feature a printed-circuit board used for both current collectors and cell connection. This latter is developed within this work.

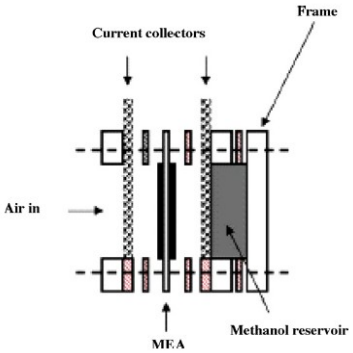

Fig. 2.6: a simple scheme of miniaturized DMFC [32]

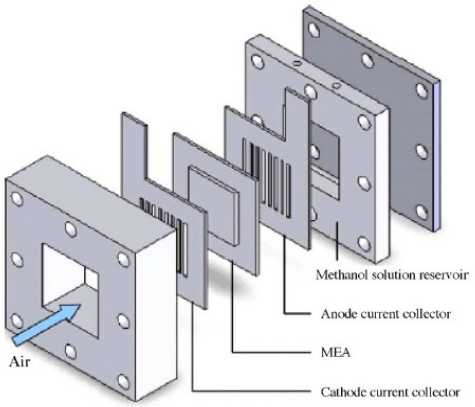

Fig. 2.7: scheme of a passive, air-breathing DMFC [34].

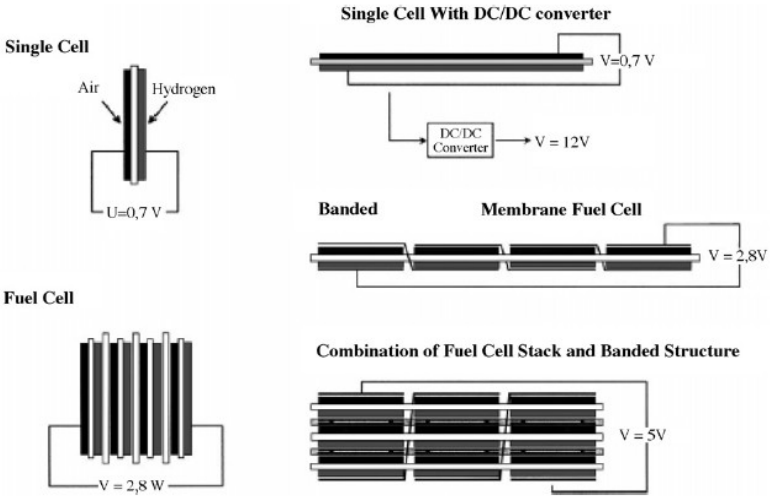

Fig. 2.8: a mixed scheme of stacked and planar configuration of miniaturized DMFC developed at Fraunhofer Institute of Solar Energy Systems [33]

2.6. References

1. Wakihara M. Recent developments in lithium ion batteries. J Mater Sci 2001; R33:109–34.

2. S. Prakash, W.E. Mustain, P.A. Kohl, Performance of Li-Ion Secondary Batteries in Low-Power, Hybrid Power Supplies, Journal of Power Sources (2008), doi:10.1016/j.jpowsour.2008.12.146

3. Goto Y. DMFC for mobile applications at Toshiba. In: Proceedings of eighth annual small fuel cells – small fuel cells for portable applications. Washington DC, USA: Knowledge Foundation; 2006 April 2–4.

4. Dyer CK. Fuel cells for portable applications. J Power Sources 2002;106(1–2):31–4.

5. Worldwide micro fuel cell market shares, strategies, and forecasts, 2009–2015. Winter Green Research; 2009

6. Stone C. Fuel cell technologies powering portable electronic devices. Fuel Cells Bull 2007;2007(10):12–5.

7. Service RF. Fuel cells: shrinking fuel cells promise power in your pocket. Science 2002; 296(17):1222–4.

8. Chang H. DMFC for note PC and mobile phone: from materials to system. In: Proceedings of eighth annual small fuel cells – small fuel cells for portable applications. Washington DC, USA: Knowledge Foundation; 2006 April 2–4.

9. Gottesfeld S. DMFC portable power products at MTI microfuel cells: present and future. In: Proceedings of seventh annual small

fuel cells – small fuel cells for portable applications. Washington DC, USA: Knowledge Foundation; 2005 April 27–29.

10. Shibata M. The latest trend of mobile fuel cells (2) – flood of new hydrogen fuel cells. In: Proceedings of the third international hydrogen & fuel cell expo, Japan; 2007. p. 1–39.

11. Jung-Ho Wee, A feasibility study on direct methanol fuel cells for laptop computers based on a cost comparison with lithium-ion batteries - Review, Journal of Power Sources 173 (2007) 424–436

12. Elizabeth Bostic, Nicholas Sifer, Christopher Bolton, Uli Ritter, Terry Dubois, The US Army Foreign Comparative Test fuel cell program. Short communication, Journal of Power Sources 137 (2004) 76–79

13. Jie-Cheng Tsai, Hui-Pin Cheng, Jen-Feng Kuo, Yao-Hui Huang, Chuh-Yung Chen, Blended Nafion(R)/SPEEK direct methanol fuel cell membranes for reduced methanol permeability, Journal of Power Sources, Volume 189, Issue 2, 15 April 2009, Pages 958-965, ISSN 0378-7753, DOI: 10.1016/j.jpowsour.2008.12.071.

14. [Yeny Hudiono, Sunho Choi, Shu Shu, William J. Koros, Michael Tsapatsis, Sankar Nair, Porous layered oxide/Nafion on nanocomposite membranes for direct methanol fuel cell applications, Microporous and Mesoporous Materials 118 (2009) 427–434

15. Jung-Ho WeeChien-Kung Lin, Jen-Feng Kuo and Chuh-Yung Chen, Preparation of nitrated sulfonated poly(ether ether ketone) membranes for reducing methanol permeability in direct methanol fuel cell applications, Journal of Power Sources, Volume 187, Issue 2, 15 February 2009, Pages 341-347

16. Y.S. Li, T.S. Zhao and Z.X. Liang, Performance of alkaline electrolyte-membrane-based direct ethanol fuel cells, Journal of

Power Sources, Volume 187, Issue 2, 15 February 2009, Pages 387-392.

17. Gang Zhang, Tiezhu Fu, Ke Shao, Xianfeng Li, Chengji Zhao, Hui Na, Hong Zhang, Novel sulfonated poly(ether ether ketone ketone)s for direct methanol fuel cells usage: Synthesis, water uptake, methanol diffusion coefficient and proton conductivity, Journal of Power Sources, Volume 189, Issue 2, 15 April 2009, Pages 875-881.

18. J.K. Lee, W. Li, A. Manthiram, Poly(arylene ether sulfone)s containing pendant sulfonic acid groups as membrane materials for direct methanol fuel cells, Journal of Membrane Science, Volume 330, Issues 1-2, 20 March 2009, Pages 73-79, ISSN 0376-7388, DOI: 10.1016/j.memsci.2008.12.043.

19. Jandee Kim, Toshiyuki Momma, Tetsuya Osaka, Cell performance of Pd-Sn catalyst in passive direct methanol alkaline fuel cell using anion exchange membrane, Journal of Power Sources, Volume 189, Issue 2, 15 April 2009, Pages 999-1002, ISSN 0378-7753, DOI: 10.1016/j.jpowsour.2008.12.108.

20. Sang-Min Park, Doo-Hwan Jung, Sang-Kyung Kim, Seongyop Lim, Donghyun Peck, Won Hi Hong, The effect of vapor-grown carbon fiber as an additive to the catalyst layer on the performance of a direct methanol fuel cell, Electrochimica Acta, Volume 54, Issue 11, 15 April 2009, Pages 3066-3072, ISSN 0013-4686, DOI: 10.1016/j.electacta.2008.11.066.

21. Yong Gao, Norman Munroe, Xiangxing Kong, Kinzy Jones, Assessing the catalyst processing for low temperature cofired ceramic-based direct methanol fuel cells, Journal of Power Sources, Volume 189, Issue 2, 15 April 2009, Pages 935-942, ISSN 0378-7753, DOI: 10.1016/j.jpowsour.2008.12.119.

22. Shengsheng Zhang, Xiaozi Yuan, Haijiang Wang, Walter Merida, Hong Zhu, Jun Shen, Shaohong Wu, Jiujun Zhang, Review, A review of accelerated stress tests of MEA durability in PEM fuel cells, International journal o f hydrogen energy, 34 (2009) 388 – 404

23. Characterization of a direct methanol fuel cell using Hilbert curve fractal current collectors, Yean-Der Kuana, Jing-Yi Chang, Shi-Min Lee, Shah-Rong Lee, Journal of Power Sources 187 (2009) 112–122

24. S. Motokawa,M.Mohamedi, T. Momma, S. Shoji, T. Osaka, Electrochem. Commun. 6 (2004) 562–565

25. A. Aravamudhan, A.R.A. Rahman, S. Bhansali, Sens. Actuators A 123–124 (2005) 497–504

26. S.K. Kamarudin, W.R.W. Daud, S.L. Ho, U.A. Hasran, Overview on the challenges and developments of micro-direct methanol fuel cells (DMFC), Journal of Power Sources 163 (2007) 743–754

27. R. Hahn, S.Wagner, A. Schmitz, H.J. Reichl, J. Power Sources 131 (2004), 73–78

28. C. Lim, C.Y. Wang, J. Power Sources 113 (2003) 145–150

29. N.I. Maluf, An Introduction to Micro-Electromechanical Systems Engineering, Artech House, London, 2000.

30. T. Pichonat, B. Gauthier-Manuel, J. Power Sources 154 (1–9) (2006), 198–201.

31. Hong Beom Park, Dewan Hasan Ahmed, Kyung Heon Lee, Hyung Jin Sung, An H-shaped design for membraneless micro fuel cells, Electrochimica Acta, In Press, Accepted Manuscript, Available online 20 March 2009, ISSN 0013-4686, DOI: 10.1016/j.electacta.2009.03.018.

32. T. Shimizu, T. Momma, M. Mohamedi, T. Osaka, S. Sarangapani, J. Power Sources 117 (2004) 277–283.

33. A. Heinzel, C. Hebling, M. Muller,M. Zedda, C. Muller, J. Power Sources 105 (2002) 250–255.

34. J.G. Liu, T.S. Zhao, Z.X. Liang, R. Chen, J. Power Sources 153 (1) (2006), 61–67.

3. Prototype basic design

3.1. System requirements

Approaching the design of a portable power supply means mostly design a simple, lightweight and compact system. The performances are sometimes sacrificed to portability features, as well as the specific cost per unit of power increases because not practically meaningful compared to other features such as reliability and lifetime. On a portable power device, the customer expects to find the same reliability, portability and usability of a battery powered device (phone, laptop, etc.). Hence a very close integration of the fuel cell power system with the portable device is needed and must be seek.

Generally a fuel cell system for portable application can be separated into three main subsystems:

- the fuel cell stack
- the fuel system
- the power electronics needed to interface the system to the load.

Fuel cell stack

The fuel cell stack for portable application must be simple to produce, should be maintenance-less during his lifetime and must operate without any customer action different from recharging or refueling. Direct methanol fuel cells (DMFC) are promising candidates for portable electric power sources because of their high energy density, lightweight, compactness, simplicity as well as easy and fast recharging [1-4]. In the last decades, a large number of publications have been focused on the development of DMFC components, such as catalysts, membranes, electrodes, etc. [5-13]. Initially, DMFC stacks have been developed as auxiliary power units (APU) or for automotive electric propulsion [14]. These stacks used a classical configuration, where single cells are stacked in series through bipolar plates. More recently, the attention has been focused on portable applications and various stack configurations have been proposed [15-20]. Thanks to integrated-circuit (IC) fabrication technology, micro-channel patterns can be featured on the silicon wafer with high resolution and good repeatability [19-21]. Moreover, in order to be commercially viable, it is important to increase efficiency and reliability. This has been achieved by eliminating power absorbed by the auxiliaries, i.e. the pump and the fan that are usually used to feed the stack with methanol and air [22 – 23]. This auxiliary-less system design is identified as “passive-feed” DMFC. It has been proposed and currently investigated by several scientists worldwide [16, 24-29].

Fuel system

The "fuel system" is the group of systems used to feed the fuel (in this case methanol) to the anode and air to the cathode. In this configuration, DMFC operate without any external device for methanol and air feeding into the cells.

At the cathode, Oxygen diffuses from the ambient to the catalytic layer due to an air-breathing action of the cell (partial pressure gradient).

At the anode, methanol can reach the catalytic layer from a reservoir driven by a concentration gradient between the electrode and the reservoir and through capillary force action of electrode pores.

Power electronic interface

The power electronic interface should accomplish the following requirements:

1. Manage the input V-I fuel cell characteristic by giving as output a power profile with constant voltage and variable current depending on load requirements and feature.
2. Monitor system status by checking, when necessary (for example at start-up, at fixed intervals or at a specified condition) the V-I characteristic of the whole system

and of each single cell to report to the customer the actual status of the system. On the base of the results achieved above, determine whether it is more convenient to operate in a different mode, i.e. bypass and disconnect a single cell, especially when its presence may result in a strong limitation of the performance of the whole system.

3. Give the designer an hardware port to check and test any sub-systems for system validation or check-up.

The use of low cost miniaturized "step-up" DC/DC converters, recently commercialized [30], increases the stack potential to a suitable, useful level with a very little dissipation of power (90% efficiency). This approach does not require intensive miniaturization of the DMFC stack, easing low cost DMFC stack design with practical electrode area.

3.2. Basic system design

The base concept of the system is a design derived from the conventional architecture of a DMFC. To simplify and reduce size of the system, most of the ancillaries have been excluded. These are the cooling loop (circuit, pumps, heat exchangers, temperature sensors and dedicated control system) and reactants feeding systems. This concept is defined as a **"passive mode"**, as the operation of the system relies mainly on a passive dynamic of the system. In a system designed to

operate in passive mode, there are many differences compared to a conventional system, as described below.

At the **cathode**, air is not forced but the the cathode is simply left exposed to ambient air. Oxygen is hence replenished by a concentration gradient from ambient to reaction sites, which results in a reduced presence of the oxidant and hence in reduced performance compared to a conventional system, where air is forced by means of a high-pressure blower. On the opposite side, there is no passive electric consumption on the system, which is one of the most passive loads for fuel cell systems. This leads to an increased overall efficiency and performance of the system operating in proper conditions.

At the **anode**, fuel is not fed by using a pump, but simply by gravity effect, positioning the tank over the system. This doesn't involve in itself any negative consequence, as fuel concentration, as a liquid, doesn't change significantly with pressure. To avoid feed issues, it must be considered that any section must be properly sized to avoid any capillary effect, caused by the presence of gas (the CO_2 produced at the anode, which moves from the anode to the fuel tank), and liquids (the fuel, which moves from the tank to the anode).

Another important difference with conventional systems, is the adoption of a planar geometry for the system, also defined “monopolar”. In this scheme, all the cathodes are on the same side of the system, as well as all the anodes are on the opposite side respect to the cathode. The cells are series-connected by

means of inner interconnections, using a conductive layer connecting an anode-cathode subsequent couple, or external connections (Fig. 3.1).

The **fuel system** must be able to feed the fuel cell stack without any active device, which power consumption might worsen the already difficult operating conditions of these systems. Theoretically, the only fuel to be replenished is methanol, although at the anode a balanced mixture of water and methanol is needed to properly operate the system. Hence in some cases a concentration sensor is used to indicate the remaining fuel. Also sensor less operation is already possible by measuring the voltage at determined operation conditions. Practically, due to water crossover from anode to cathode, sometimes it might be preferably to change the whole fuel tank (often in the form of a removable cartridge) and hence replenishing the whole water-methanol mix into nominal conditions.

Another issue to consider, when designing such a system, is that the system is sensible to its geometrical orientation, as well as to shakes, shocks and rollovers. All these issues have negative consequence on the operation of the system and proper countermeasures should be always considered whenever possible.

At **system** level, the system is intended to operate at ambient conditions, hence the temperature is no more controlled. This assumption has the consequence to decrease overall

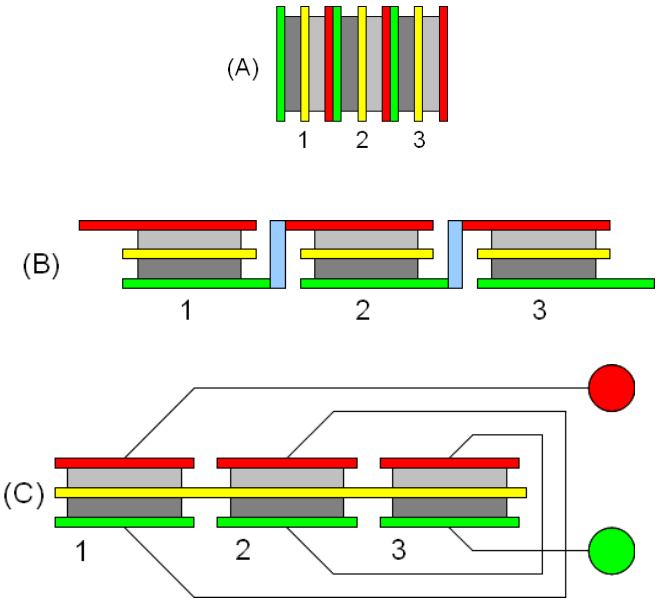

Fig. 3.1.: solutions for a planar system compared to a conventional stack (A): a planar configuration with internal interconnections (B) and with external interconnections (C).

performance, as performances increase with temperature. Considering the low power generated by these systems and the large surface exposed to ambient air, the heat generated by the system is not sufficient to warm up the system and rise the temperature to the optimal level typical of DMFC (usually close to 130°C), hence the operating temperature is only slightly higher than ambient*. Moreover, the system must be designed to manage passively the heat exchange with ambient, avoiding any overheating possibility. Considering the need of compactness, robust and reliability, as well as the very limited power of the system, the overheat issue might be simply managed by a a shut-down switch regulated from a simple temperature sensor.

3.3. Stack design

The system has been designed to operate in passive mode, with the fuel tank directly attached to the anode side. It is a three

* An overheating of a passive planar system is often an indication of a massive fuel crossover. Due to crossover, fuel migrates from anode to cathode through the electrolyte membrane and it is locally oxidized at the cathode without producing any current. The whole enthalpy is converted into heat and a local overheating is easily detected, with temperature often in the 50-80 °C range, operating at ambient conditions with liquid fuels such as Methanol.

cell planar stack (Fig. 3.2), externally connected in series to simplify single cell testing.

The hardware has been derived from a PCB board, properly machined to accommodate all the needed subsystems, i.e. air and fuel inlets, electrical connections, tightening bolts, sealing, MEA, fuel tank and, in principle, the electronic systems, which hasn't been included yet because final specification where not known yet. The fuel reaches the anode from the tank to the anode through 1 mm diameter holes machined into the PC plate. The contacts between the electrodes and the board are gold plated to avoid oxidation and corrosion issues due to the strong methanol activity. The electric circuit is covered by an electric protection paint (the green cover visible in Fig. 3.2).

3.4. MEA design and realization

The electrodes for a three-cell stack were composed of commercial gas-diffusion layer-coated carbon cloth for high temperature (HT-ELAT, E-TEK) and low temperature operation (LT-ELAT, E-TEK) at the anode and cathode, respectively. Unsupported Pt–Ru (Johnson-Matthey) and Pt (Johnson-Matthey) catalysts were mixed with 15 wt.% Nafion ionomer (Ion Power, 5 wt.% solution) and deposited onto the backing layer for the anode and cathode, respectively. Nafion117 (Ion Power) was used as electrolyte. The MEA for a monopolar mini-stack (three cells) was made by assembling simultaneously three sets of anode and cathode pairs on each

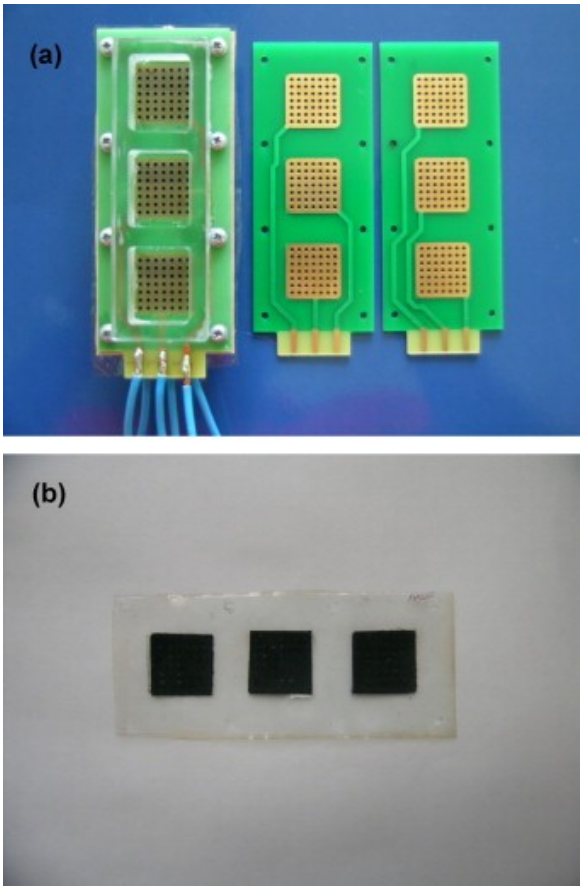

Fig. 3.2. photos of the DMFC three-cell stack with the monopolar plates (a) and MEA formed by a single membrane and three couples of electrodes (b).

side of the membrane and then sandwiched between two plastic plates covered by thin gold film current collectors in the area of electrodes with a distribution of holes through which methanol (from a reservoir) and air (from ambient) could diffuse into the electrodes. The active area of each electrode was 4 cm^2 and the total active area of the stack was 12 cm^2. Series connections between the cells were made externally through the electric circuit. A picture of the device is reported in Fig. 3.2a. Fig. 3.2b shows the complete membrane-electrode assembly for the mini-stack incorporating a single membrane and three couples of electrodes.

3.5. Test and evaluation of the prototype.

At this stage, an optimization of properties and operating parameters of a passive direct methanol fuel cell monopolar stack is performed, such as methanol concentration and catalyst loading. The influence of Pt loading, already investigated in a conventional forced-flow DMFC [31], was analyzed under passive operation, taking into account the mass transfer constraints caused by the needed high catalyst loading.

Catalyst and fuel concentration influence

Different Pt loadings were evaluated in order to investigate the effect of catalytic layer thickness on the electrochemical behavior of the air breathing monopolar stack. A small catalyst

loading is associated to a small electrode thickness. This helps an easier access of the reactants to the reaction region (electrode–electrolyte interface) and thus lower mass transfer constrains but there is also a small number of catalytic sites. A Pt loading ranging from 1.5 to 6 mg cm^{-2} for both anodes and cathodes was investigated. Different methanol concentrations from 1 M up to 10 M were evaluated. The stack was operating under passive mode at room temperature (21 ± 2 °C). No auxiliaries such as pumps, heaters, humidifiers or blowers were used. In this passive mode, oxygen molecules spontaneously diffuse into the cathode (air-breathing effect). Such a phenomenon is induced by the concentration gradient at the electrode–electrolyte interface where oxygen is consumed by the electrochemical reaction. Similarly, methanol diffuses from the tank, attached to the anode compartment (see Fig. 3.2a), to the electrode by effect of the concentration gradient caused by the electrochemical consumption of fuel. Performances were investigated by steady-state galvanostatic polarizations and chrono-potentiometric measurements using an AUTOLAB PGSTAT 302 Potentiostat/Galvanostat (Metrohm).

The polarization and power density curves for the three-cell stack equipped with electrodes containing 1.5 mg cm^{-2} Pt loading on both sides and different methanol concentrations placed in the reservoir (1 M, 2 M and 5 M) are shown in Fig. 3.3. The thickness of the total anode electrode (catalytic, diffusion and backing layers), calculated by SEM (not shown), was 370 μm; whereas, it was 300 μm for the cathode. An open circuit voltage (OCV) higher than 2 V was recorded with 1 M

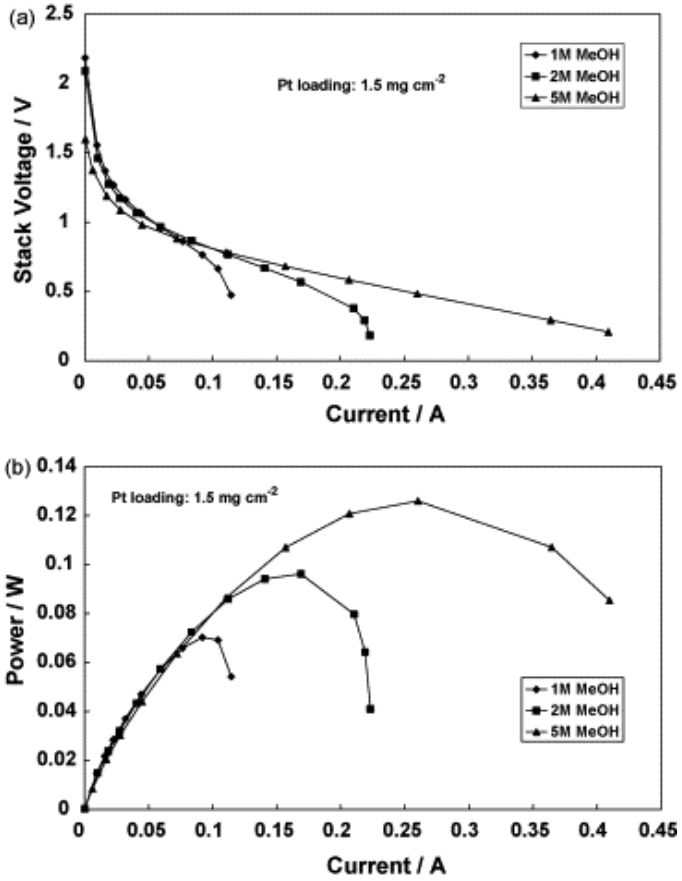

Fig.3.3: Polarization (a) and power (b) curves for the three-cell stack with a Pt loading of 1.5 mg cm^{-2} on each electrode at different methanol concentrations.

and 2 M methanol solutions; whereas, it decreased to 1.6 V with the concentrated solution (5 M). In particular, the OCV obtained with 1 M was higher than that with 2 M, indicating, as expected, a larger methanol cross-over through the membrane as the fuel concentration was increased. It is pointed out that a continuous single membrane sheet is used; thus, the membrane is not interrupted at the border between each cell. Accordingly, the methanol permeation is not substantially different from that of a single cell of similar membrane area.

The same trend of the OCV was observed for the voltage as a function of methanol concentration at low current; whereas, increasing the current, the stack voltage decreased rapidly with 1 M methanol (diffusion limiting current of about 120mA), less significantly with 2M (diffusion limiting current of about 225mA), reaching more than 400mA with 5M methanol solution. It is derived that at low fuel concentrations the process is controlled at high currents by the methanol mass transport process, i.e. the limiting current increases twice as the methanol concentration in the reservoir passes from 1M to 2M at potential as high as 0.5V. Whereas, such a linear increase of limiting current is not so strictly observed for 5M methanol solution since at potentials as low as 0.2V the recorded value is 4 times less than that measured with 1M concentration. Obviously, in the latter case, there is the effect of cross-over that is reflected in the overall range of current density. Furthermore, it is not excluded that increasing methanol concentration, some kinetics constrains may arise from a reduced rate for the water discharging [8].

Thus, the mass transfer control, corresponding to the methanol concentration of 5M, is not achieved in the practical range of stack voltage. Yet, an important fact is that under conditions where mass transport plays an important role (passive mode), a significant increase of methanol concentration causes an increase of output power. This effect, combined to the better energy density, makes operation at high concentration quite interesting even in the absence of specific tools that help water back diffusion from cathode to the anode [32].

A maximum power of 120mW was reached with the most concentrated solution. Using a diluted solution at the anode, as above discussed, the maximum power was smaller than that obtained with a concentrated solution due to mass transfer limitations. Under practical operation the "step-up" DC/DC converter should allow the stack potential to remain in a suitable range with a small power dissipation.

Performance evaluation

An investigation of the electrochemical performance of each cell in the stack was carried out for the electrodes with 1.5 mg cm^{-2} Pt loading, using 2 M methanol solution at the anode (Fig. 3.4). The three cells showed a slightly different behavior. Cell 1 (which was closer to the end current collector) appeared to be more performing than the other cells. This is due to the lower cell resistance for this cell (0.64Ω cm^2) compared to the other ones that are more distant from the end current collector (0.7Ω

cm^2 for cell 2 and 0.8Ω cm^2 for cell 3). The obtained maximum power density and short circuit current density are affected by these values of cell resistance; in fact, higher current and power densities were reached with cell 1 (a maximum power density of 10mW cm^{-2}); whereas, cells 2 and 3 showed lower performance (7 and 6.5mW cm^{-2}, respectively). The performance of the three cells in such a monopolar configuration thus reflects the location of each cell with respect

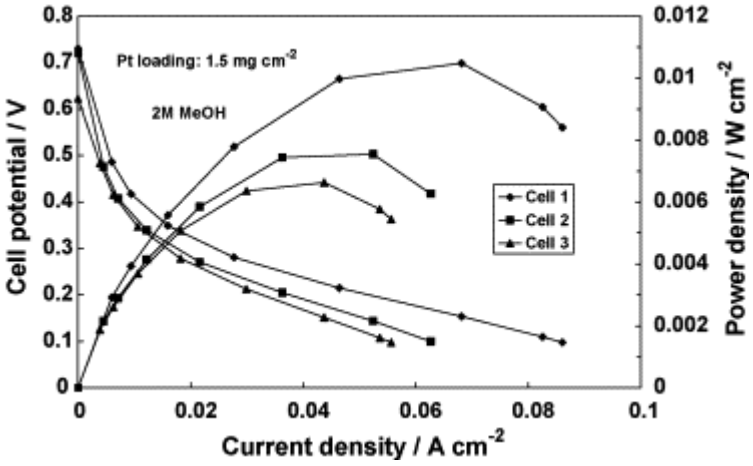

Fig. 3.4. Polarization and power density curves for each cell of the stack with a Pt loading of 1.5mg cm^{-2} using 2M methanol solution.

to the external electronic circuit that allows series connection between them.

A stability test of 1 h of continuous operation was carried out on the three-cell stack equipped with electrodes containing 1.5mg cm^{-2} Pt loading at a voltage of 0.9V using 20 vol.% methanol solution (Fig. 3.5). A slight decrease of current was observed with a concentrated solution of methanol, probably due to the large swelling of the membrane causing an increase of methanol cross-over, which results in a decrease of performance with time. Furthermore, due to an excess of methanol/water coming from the anode, also promoted by the electro-osmotic drag, a flooding of the cathode catalytic layer could be responsible of such a decrease of current. Increasing the Pt loading (4mg cm^{-2} on both sides), the performance increased significantly at all conditions and it was almost twice in terms of maximum power (225mW) with a methanol concentration of 5 M compared to the stack based on 1.5mg cm^{-2} Pt loading (120mW); whereas, the OCV remained the same. The largest gain appeared to be achieved with 2M methanol concentration. The performance with 2M was approaching that of 5M methanol solution. The limiting current density was practically the same for 1M methanol, whereas it slightly increased for 2M and 5M methanol solutions (Fig. 3.6).

At high methanol concentration no mass transfer control was observed in the practical stack voltage range. The gain in performance was not strictly proportional to the increase of catalyst loading. This is possibly due to the fact that the

extension of the three-phase reaction zone is not proportional to the increase of the electrode thickness (400μm for the anode, 325μm for the cathode). Mass transfer constrains influence the behavior, especially if a diluted methanol solution (1M) is used. The trend of the OCV and voltage at low current (in the activation region) is the following: 1M ≥ 2M > 5M.

At intermediate current, under 2M and 5M methanol concentration at the anode (passive mode), the behavior was similar, even if slightly higher performances were recorded with the diluted solution (2M) probably due to the lower

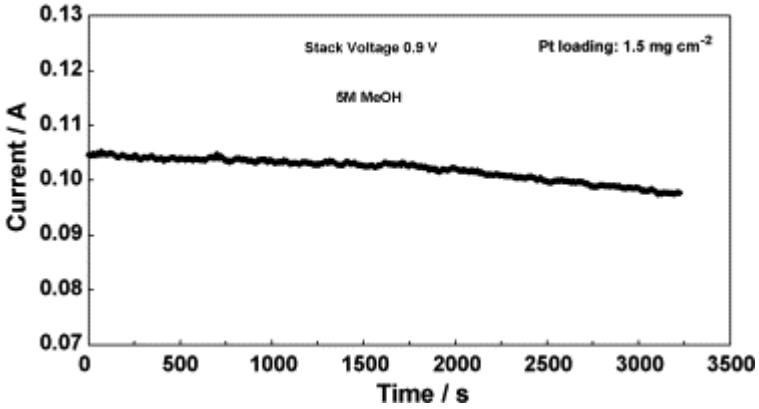

Fig. 3.5. Chrono-amperometric experiment carried out on the stack with a Pt loading of 1.5 mg cm^{-2} on each electrode at 0.9 V using 5 M methanol solution.

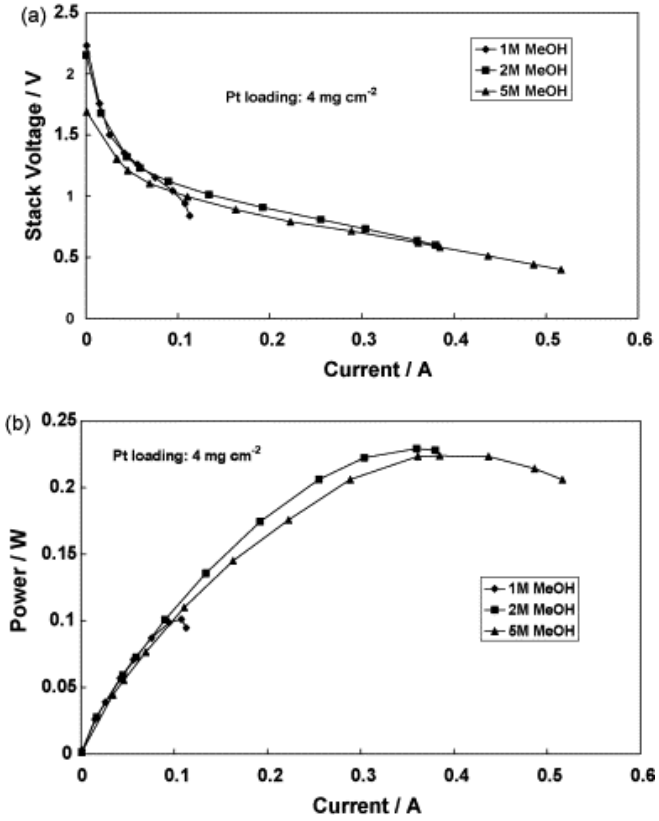

Fig. 3.6. Polarization (a) and power (b) curves for the three-cell stack with a Pt loading of 4 mg cm^{-2} on each electrode at different methanol concentrations.

methanol cross-over. At high current, the situation was the opposite and the concentrated solution gave rise to lower voltage losses. In this latter case, although no limiting current was reached, the mass transfer plays a significant role.

A time stability test of 1 h was carried out also under these conditions (Fig. 3.7) at a voltage of 0.9V using 5M methanol solution. Also in this case, a slight decrease of performance was observed as a function of time, but lower than that

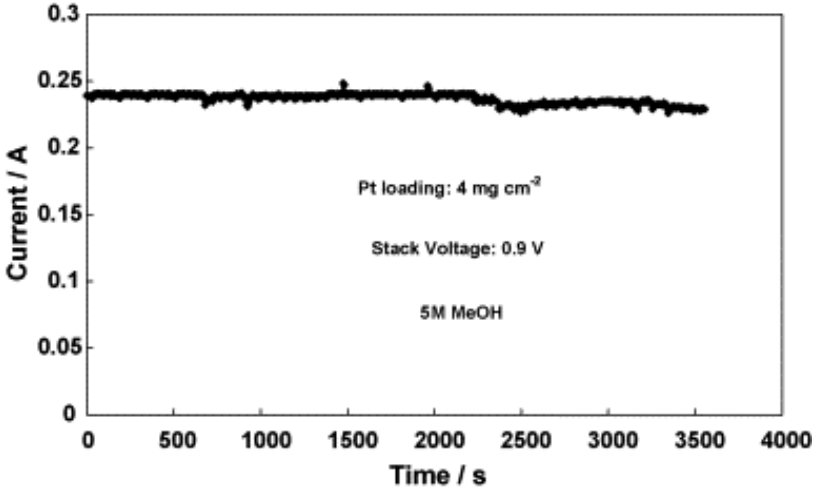

Fig. 3.7. Chrono-amperometric experiment carried out on the stack with a Pt loading of 4 mg cm−2 on each electrode at 0.9 V using 5 M methanol solution.

recorded with a lower amount of Pt in the electrodes. This may be ascribed to two effects, i.e. anode thickness, which reduces the methanol cross-over rate by increasing the tortuosity factor for permeation, and the increased amount of catalyst (thickness) at the cathode counteracts the effects of poisoning by methanol. A further increase of Pt loadings (6 mg cm^{-2}) produced a significant increase of mass transport constrains (the thickness in this case was 420μm for the anode and 340μm for the cathode), in particular with low methanol concentrations (1 and 2M).

Well defined limiting current densities were measured at stack voltages above 0.6V. The increased thickness of the reaction layer hinders the reactants to reach the active zone at the electrode-membrane interface, where most of the reaction process occurs. This effect agrees with the fact that the extension of the three-phase reaction zone is not proportional to the thickness of the catalytic layer. The behavior of the stack equipped with electrodes containing 6mg cm^{-2} Pt loading on both compartments (Fig. 3.8) in the activation and ohmic controlled regions was similar to that recorded with lower amount of catalyst; whereas, the maximum current reached in these conditions was lower than that obtained in the previous experiment carried out using 4mg cm^{-2} Pt content. By comparing the polarization and power density curves recorded with different Pt loadings (Fig. 3.9), it is derived that the best performance in terms of power and current output is achieved with 4mg cm^{-2} Pt loading on both compartments that represents

the best compromise between amount of catalytic sites and thickness.

Yet, the OCV and voltage at low currents (activation region) was slightly higher using a larger catalyst content as a consequence of reduced cross-over and large number of active sites. Indeed, diffusion constrains occur at high currents during passive mode operation due to the thickness of the electrodes.

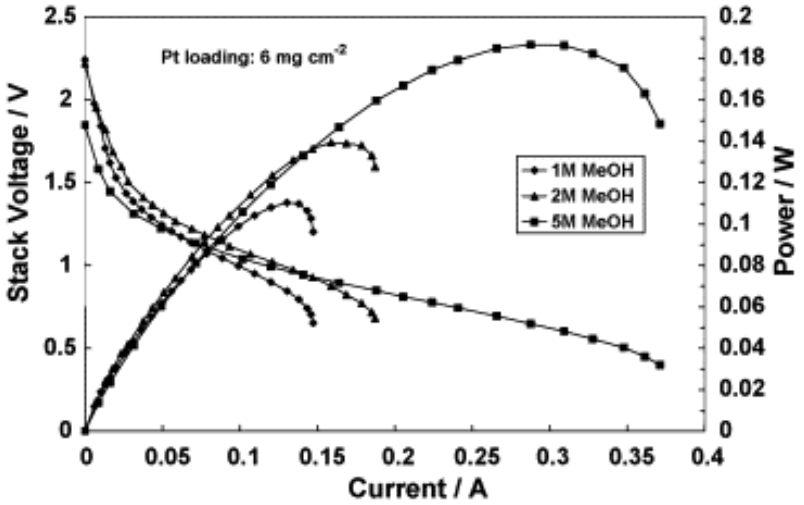

Fig. 3.8. Polarization and power curves for the three-cell stack with a Pt loading of 6 mg cm−2 on each electrode at different methanol concentrations.

By increasing the methanol concentration up to 10M, the performance decreased (Fig. 3.10) due to the large swelling of the membrane that produces a higher methanol cross-over. A comparison of the polarization profile of the stack fed with 5M and 10M concentrations shows that there is a significantly different OCV due to the increased cross-over with 10M concentration (in the absence of electro-osmotic drag); this voltage loss is reflected on the overall polarization curve.

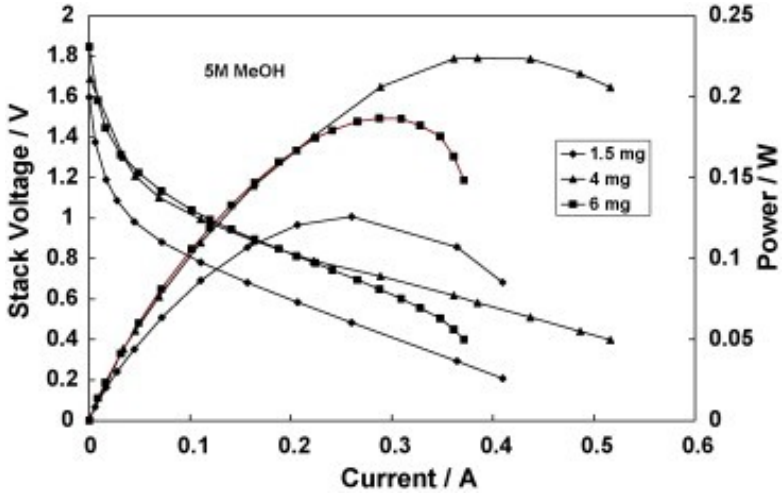

Fig. 3.9. Comparison of the polarization and power curves for different stacks varying by the Pt loading on each electrode and using 5 M methanol solution at the anode.

Whereas, the extent of activation losses up to 0.1A is quite similar. This suggests that the development of alternative membranes with similar conductivity but significantly smaller cross-over than Nafion may allow to achieve in the presence of highly concentrated methanol solutions the same power density obtained for diluted methanol concentrations (5M). The necessary water for anode reaction to occur can reach the anode/electrolyte interface by back diffusion from the cathode as demonstrated in literature [32].

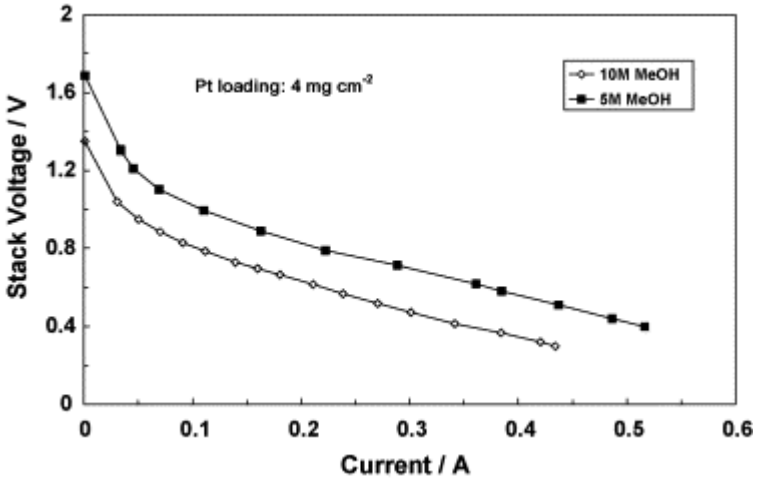

Fig. 3.10. Comparison of the polarization curves for the three-cell stack with a Pt loading of 4 mg cm−2 on each electrode at high methanol concentrations (5 M and 10 M).

Further experiments were carried out in order to evaluate the effect of variation of Pt loading at the anode and cathode, separately. For this purpose, in a new MEA, a Pt loading of 4mg cm−2 at the anode and 1.5mg cm^{-2} at the cathode was used; in another MEA the loading was 1.5mg cm−2 at the anode and 4mg cm−2 at the cathode. Fig. 3.11 reports a comparison of the polarization curves obtained with these new MEAs together with those of the MEAs equipped with 1.5mg cm^{-2} or 4mg cm^{-2} Pt loading on both electrodes. Such a comparison is presented for a methanol concentration of 5M.

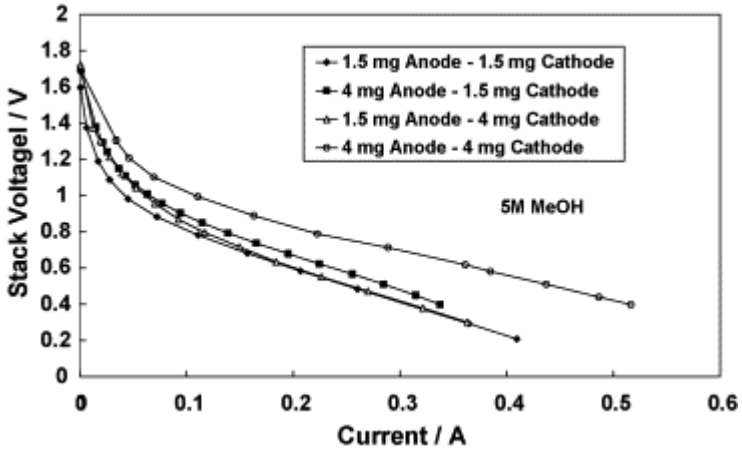

Fig. 3.11. Comparison of the polarization curves for the stacks varying the Pt loading at the anodes and cathodes, using 5 M methanol solution.

An increase of performance in the activation region was observed for the two new MEAs with respect to the cell based on 1.5mg cm^{-2} Pt loading on both electrodes. This is due to the increased amount of catalytic sites for methanol oxidation and oxygen reduction when a higher loading at the anode or at the cathode (4mg cm^{-2}) is used. Thus, both electrochemical processes appear to limit the stack performance.

The increase in potential is reflected in the whole polarization curve only for the anode with high loading. Obviously, the performance of this cell is inferior to that of the cell equipped with 4mg cm^{-2} Pt loading on both compartments. This is due to the cross-over effect that causes a poisoning of the reaction sites for the ORR on the cathode (taking into account the low Pt loading, 1.5mg cm^{-2}). The higher performance in the activation region of the MEA equipped with 1.5mg cm^{-2} at the anode and 4mg cm^{-2} at the cathode compared to the MEA based on 1.5mg cm^{-2} Pt loading on both electrodes could be attributed to the large availability of catalytic sites at the cathode (4mg cm^{-2} Pt loading) that counteracts the detrimental effect of methanol cross-over. Yet, in this case, an increase of Pt loading at the cathode causes an increase of electrode thickness. This, in turn, produces an increase of mass transport constrains at high currents. Thus, for the air breathing process, a compromise between the number of catalytic sites and the electrode thickness is necessary.

For what concerns the methanol cross-over, due to the fact that no air flow at the cathode is used, the well-established CO_2

sensor method is not applicable. Alternatively, electrochemical determination of methanol passed at the cathode by measuring the methanol oxidation current at the cathode in the presence of an inert gas does not appear appropriate. This method discards the effects of operating current density (concentration gradient at the anode–electrolyte interface) and electro-osmotic drag. Thus, we have evaluated the cross-over rate on the basis of the Faradaic efficiency determination (fuel efficiency) when all methanol in the tank was consumed (before re-fuelling). This approach is based on the assumption that the reduction of Faradaic efficiency from the ideal 100% is only due to the methanol loss by the cross-over through the membrane. Our chromatographic analysis of the methanol solution in the tank showed no organic compounds other than methanol and CO_2 at the anode compartment during operation. Particular care was addressed to reduce any methanol loss from the tank by evaporation. From this analysis, a total methanol cross-over rate in the stack of $1.5 \pm 0.2 \times 10^{-6}$ mol min^{-1} cm^{-2} (total geometric electrode area) at 21 °C was determined under passive mode operation with 5M MeOH, 4mg Pt loading on both electrodes and 60mA cm^{-2} operating current density.

3.6. Conclusions

In this stage, a characterization of a passive DMFC monopolar stack was carried out, varying the catalyst loading and methanol concentration. From this analysis, it is derived that

4mg cm^{-2} Pt loading in the presence of unsupported catalysts appears to be the best compromise between electrode thickness and amount of catalytic sites for suitable mass transport and kinetics of anode and cathode reactions, in particular using a methanol concentration ranging from 2M up to 5M. A maximum power of 225mW was obtained at ambient temperature for the three-cell stack with 4mg cm^{-2} Pt loading on each electrode using both 2M and 5M methanol concentration at the anode, corresponding to a power density of about 20mW cm^{-2}. The use of highly concentrated methanol solutions causes a significant decrease of OCV that reflects on the overall polarization curve; however, the activation losses are similar. This strongly suggests the development of proper methanol impermeable membranes.

Under the design and the engineering point of view, the system architecture has shown acceptable features in terms of electric resistance, which is lower than that of conventional system with graphite stacked plates. Sealing has been realized using two overlapping sheets of Gore-Tex® 1 mm thick expanded PTFE membrane (Fig. 3.12). This sealing has very good performances and adaptability to the surface of the PCB but the need of a double layer (one on each side of the membrane), obtained by overlapping two 1 mm thick sheets, resulted in a excessive thickness, despite the material wide adaptability in terms of thickness reduction under pressure (higher than 50%): sometimes this resulted in the loss of electrical contact between the collector and the electrodes. By hot-pressing the seal within the PCB and the MEA, before applying the bolts and the tank,

the thickness can be further reduced and the assembly is more stable but the assembly process becomes more complex.

Using a two-fold layers of a different fiber-reinforced sealing polymer, as shown in Fig. 3.13, the contact issue has been solved, although some leakage from the PCB outer perimeter has been detected in some cases due to electrolyte membrane swelling. The issue has been removed by re-assembling the stack. Unfortunately at the moment it was not possible to find any other alternative because of available standards and market availability in very small quantities.

The stack design has shown to be reliable and easy to manufacture. The PCB design is a very well established technology and a fast process which can be up-scaled to produce thousands of devices at a very low cost. Continuous changes of MEA and maintenance operations during the testing activity caused a partial detach of the gold plate over the electric collector in the electrode zone. This issue is considered acceptable considering that in normal operation the stack should not be opened unless strictly necessary (i.e. fault of the MEA). The stack testing has shown a design limitation. At the anode, where a 1,5mm holed mesh is used to feed the fuel to the anode, the CO_2 produced during methanol oxidation remains entrapped within the PCB-anode interface. This effect blocks the fuel migration to the anode, hence the stack shows the typical behavior of a system which runs out of fuel. This happens because the consumed fuel is not replenished from that in the tank due to bubbles blocking the access to the

Fig. 3.12: Gore-Tex ® expanded PTFE sealing for the three cell planar stack. There are visible the three electrodes (in black), meanwhile the sealing is the white frame around the electrodes.

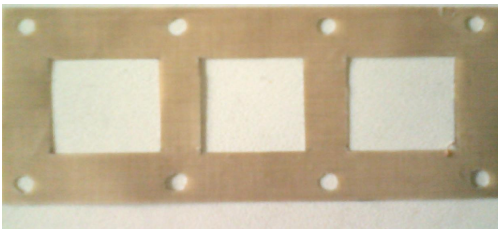

Fig. 3.13: fiber reinforced sealing polymer used to seal the three cells planar stack.

electrode. It happens much before the fuel is effectively consumed from the tank. This issue, already addressed by other authors, limits the autonomy of the system unless CO_2 bubbles are mechanically removed (by agitation) or unless the bubble size is large enough to leave the reaction site. A similar issue is also present at the cathode, which features a similar mesh. There, water and fuel crossover cause a flooding effect, preventing oxygen (air) to reach the reaction sites and hence rapidly degrading stack performance.

These issues have been addressed by redesigning the stack as discussed in the next chapter.

3.7. References

1. C.K. Dyer, J. Power Sources 106 (2002), p. 31.

2. R. Dillon, S. Srinivasan, A.S. Aricò and V. Antonucci, J. Power Sources 127 (2004), p. 112.

3. M. Neergat, D. Leveratto and U. Stimming, Fuel Cells 2 (2002), p. 25.

4. S. Gottesfeld, Fuel Cells 5 (2005), p. 45.

5. X. Ren, M.S. Wilson and S. Gottesfeld, J. Electrochem. Soc. 143 (1996), p. L12.

6. A.K. Shukla, P.A. Christensen, A.J. Dickinson and A. Hamnett, J. Power Sources 76 (1998), p. 54.

7. S. Wasmus and A. Kuver, J. Electroanal. Chem. 461 (1999), p. 14.

8. A.S. Aricò, S. Srinivasan and V. Antonucci, Fuel Cells 1 (2001), p. 133.

9. C. Coutanceau, R.K. Koffi, J.-M. Leger, K. Marestin, R. Mercier, C. Nayoze and P. Capron, J. Power Sources 160 (2006), p. 334.

10. W.J. Zhou, B. Zhou, W.Z. Li, Z.H. Zhou, S.Q. Song, G.Q. Sun, Q. Xin, S. Douvartzides, M. Goula and P. Tsiakaras, J. Power Sources 126 (2004), p. 16.

11. A. Oedegaard, C. Hebling, A. Schmitz, S. Moller-Holst and R. Tunold, J. Power Sources 127 (2004), p. 187.

12. A.S. Aricò, V. Baglio, A. Di Blasi, E. Modica, P.L. Antonucci and V. Antonucci, J. Electroanal. Chem. 557 (2003), p. 167.

13. V. Baglio, A.S. Aricò, A. Stassi, C. D'Urso, A. Di Blasi, A.M. Castro Luna and V. Antonucci, J. Power Sources 159 (2006), p. 900.

14. D. Buttin, M. Dupont, M. Straumann, R. Gille, J.-C. Dubois, R. Ornelas, G.P. Fleba, E. Ramunni, V. Antonucci, A.S. Aricò, E. Modica, M. Pham-Thi and J.-P. Ganne, J. Appl. Electrochem. 31 (2001), p. 275.

15. A. Heinzel, C. Hebling, M. Muller, M. Zedda and C. Muller, J. Power Sources 105 (2002), p. 250.

16. D. Kim, E.A. Cho, S.-A. Hong, I.-H. Oh and H.Y. Ha, J. Power Sources 130 (2004), p. 172.

17. T. Ito, K. Kimura and M. Kunimatsu, Electrochem. Commun. 8 (2006), p. 973.

18. A. Blum, T. Duvdevani, M. Philosoph, N. Rudoy and E. Peled, J. Power Sources 117 (2003), p. 22.

19. S.C. Kelley, G.A. Deluga and W.H. Smyrl, Electrochem. Solid State Lett. 3 (2000), p. 407.

20. G.Q. Lu, C.Y. Wang, T.J. Yen and X. Zhang, Electrochim. Acta 49 (2004), p. 821.

21. G. D'Arrigo, C. Spinella, G. Arena and S. Lorenti, Fuel Cells Bull. 4 (2003), p. 10.

22. H. Yang, T.S. Zhao and Q. Ye, J. Power Sources 139 (2005), p. 79.

23. G.Q. Lu and C.Y. Wang, J. Power Sources 134 (2004), p. 33.

24. J. Bostaph, R. Koripella, A. Fisher, D. Zindel and J. Hallmark, Proceedings of the 199th Meeting on Direct Methanol Fuel Cells, Electrochemical Society Washington, D.C., USA, March 25–29 (2001).

25. G. Jewett, Z. Guo and A. Faghri, J. Power Sources 168 (2007), p. 434.

26. R. Chen and T.S. Zhao, J. Power Sources 167 (2007), p. 455.

27. R. Chen and T.S. Zhao, Electrochim. Acta 52 (2007), p. 4317.

28. R. Chen and T.S. Zhao, Electrochem. Commun. 9 (2007), p. 718.

29. M.A. Abdelkareem and N. Nakagawa, J. Power Sources 165 (2007), p. 685.

30. www.maxim-ic.com.

31. V. Baglio, A. Di Blasi, E. Modica, P. Cretì, V. Antonucci and A.S. Aricò, J. New Mater. Electrochem. Syst. 9 (2006), p. 41.

32. S. Gottesfeld, J. Power Sources 171 (2007), p. 37.

4. Revised design

4.1. Introduction

In a passive fuel cell, as discussed in the previous chapters, oxygen diffuses into the cathode from ambient due to an air-breathing action of the cell and without any external devices such as a fan. The oxygen partial pressure gradient is directly increased by oxygen consumption. Similarly, the methanol solution, stored in the reservoir attached to the anode plate, diffuses into the anode driven by a concentration gradient between the reservoir and anode, as a consequence of electrochemical consumption. Hence it is a crucial issue to properly design the cathode and anode inlets to ease reactant flow.

Passive DMFC can potentially result in high reliability, low cost, high fuel utilization and high energy density (using a concentrated methanol solution), which makes them suitable for portable equipments in forecoming electronic devices [1-3]. A significant amount of work has been reported on passive DMFCs, such as investigations of the optimal fuel concentration, membrane thickness, membrane–electrode assembly (MEA) fabrication and optimization, etc. [4-14], but

limited attention has been focused on the influence of the flow field/current collectors on the performance and discharge behavior of passive DMFC stacks. As seen at the end of the previous chapter, these aspects can not be ignored, otherwise resulting in a heavy performance limitations. In the present chapter, a comparison between two designs of flow fields/current collectors for a three-cell passive DMFC monopolar stack is presented. An investigation of the performance and discharge behavior of the two designs was carried out by analyzing advantages and disadvantages of each configuration.

4.2. Definition of the improved design

Two designs for a three-cell stack were realized. Both feature PCB plates incorporating the electric circuitry and current collectors for anode and cathode. The difference relates in the current collector design and in some other solutions tested at the electrode-collector interface. The two designs have been tested and compared, identified simply as design “A” and “B”.

The first design (design A) is the one already tested in the previous chapter. It features two printed circuit boards (PCBs) covered by thin gold film current collectors in the area of electrodes. There a mesh of 1,5 mm holes allows methanol (from a reservoir) and air (from ambient) diffusion to the electrodes (Fig. 4.1).

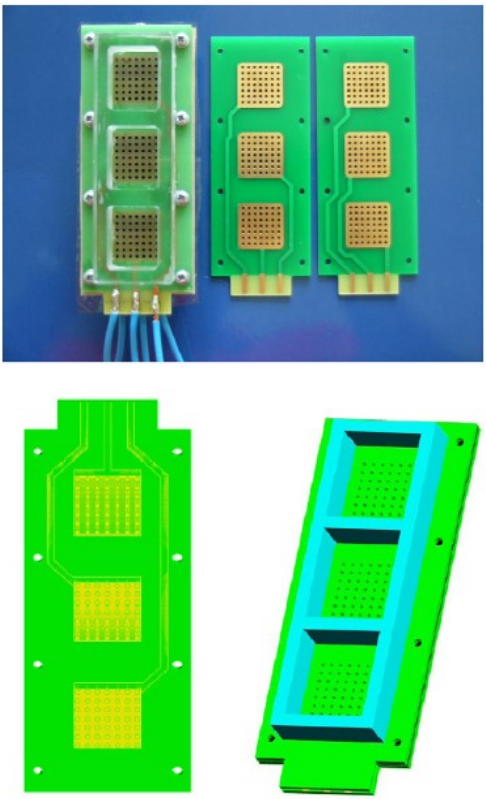

Fig. 4.1: 3D model (below) and the realization (above) of the design “A” DMFC three-cell passive stack with the monopolar plates.

The second design (design B) is similar to design A in terms of materials employed, but there is no specific flow field or mesh for liquid and gas diffusion into the housing of the monopolar stack. The current collectors are made of a thin gold film deposited on the external borders of the fuel and oxidant apertures where the electrodes were placed in contact (Fig. 4.2). In this design, the central part of the electrode is exposed directly to the ambient air (for the cathodes) and methanol solution (for the anodes). The two plates (for the anodes and cathodes) were assembled as shown in Fig. 4.3. The geometrical electrode area was the same for the two designs and it was considered for the calculation of power and current density. It resulted from both electrode regions exposed to fuel/oxidant and in contact with the current collector. A methanol reservoir (containing in total 21ml of methanol solution, divided in three separate compartments), with 3 small holes in the upper part to fill the containers and to release the produced CO_2, was attached to the anode side. The electrodes were composed of a commercial coated gas diffusion layer made in carbon cloth, namely HT-ELAT and LT-ELAT (E-TEK) at the anode and cathode respectively. Unsupported Pt–Ru (Johnson-Matthey) and Pt (Johnson-Matthey) catalysts were mixed with 15 wt.% Nafion ionomer (Ion Power, 5 wt.% solution) and deposited onto the backing layer for the anode and cathode, respectively. Nafion 117 (Ion Power) was used as electrolyte.

The MEAs for the two stack designs (three cells) were manufactured by assembling simultaneously three sets of

anode and cathode pairs on each side of the membrane and then sandwiched between the two PCBs. The geometrical area of each electrode was 4cm^2 and the total area of the stack was

Fig. 4.2: design “B” of the three cell planar stack. The holed mesh has been removed, leaving a gold-plated peripheral frame acting as current collector to ensure contact between the electrode and the circuit.

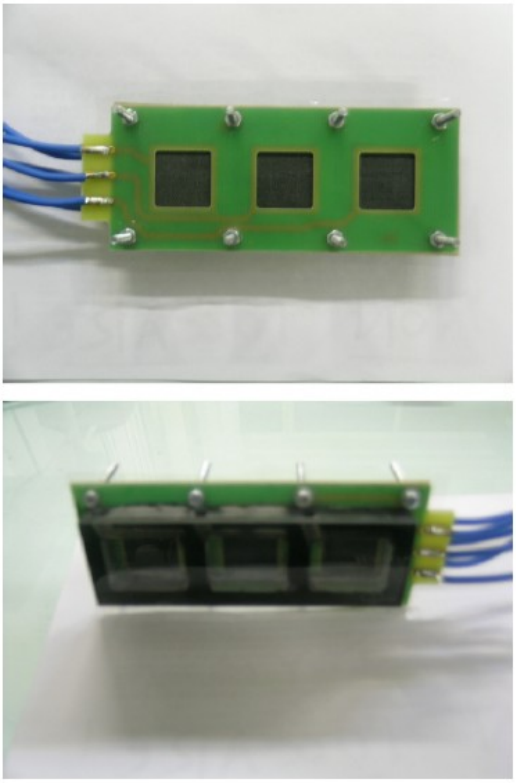

Fig. 4.3: the planar monopolar stack assembled. The above image shows the three cathode set, directly exposed to ambient air. In the image below it is visible the fuel tank assembled directly over the PCB board and the three anode set, directly in contact with the methanol solution.

12cm^2. Series connections between the cells were made externally through the electric circuit. Fig. 4.4 shows the complete membrane–electrode assembly for the two mini-stacks formed by a single membrane and three couples of electrodes.

A Pt loading, ranging from 1.5 to 6 mg cm^{-2} , was investigated using the design A of the stack. Afterward, the optimal Pt loading was used to investigate the behavior of the two stack designs. Methanol concentrations of 2 and 5M were used in the experiments. The stack was operating under passive mode at room temperature (21 ± 2 °C). Performances were investigated by steady-state galvanostatic polarizations and chrono-potentiometric measurements by using an AUTOLAB PGSTAT 302 Potentiostat/Galvanostat (Metrohm) equipped with a FRA (Frequency Response Analyzer). The ohmic drop was

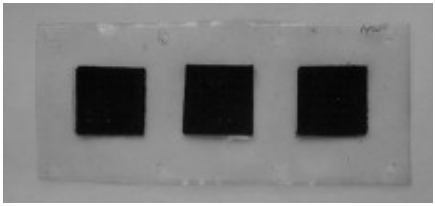

Fig. 4.4: the three electrode MEA assembled. The membrane is a continuous single sheet, which makes MEA easier to assemble within the stack but also increases crossover from the outer zones.

determined by measuring the high frequency impedance at null current.

4.3. System testing and performance evaluation

An investigation of the optimal catalyst loading for a low temperature DMFC was already carried out in [15] with a forced flow single cell. The influence of catalyst loading was also investigated under passive mode by using the design A of the mini-stack. A low catalyst loading is associated to a little electrode thickness. This allows the reactants an easier access to the reaction region (electrode–electrolyte interface) with a consequent decrease of the mass transfer constraints. Such aspects are more relevant for the passive mode operation as compared to the forced flow conditions. Yet, a small number of catalytic sites may limit the kinetics of the electrochemical reactions producing low performances. Fig. 4.5 shows a comparison of the polarization and power curves at different Pt loadings. It is derived that the best performance in terms of power and current out put is achieved with 4mg cm^{-2} Pt loading. This represents the best compromise between the number of catalytic sites and thickness. Yet, the open circuit voltage (OCV) and stack voltage at low currents (activation region) was slightly higher using a larger catalyst content (6mg cm^{-2} on both compartments) as a consequence of reduced cross-over (a thicker anode reduces the methanol permeation [11]) and large number of active sites. Indeed, diffusion

constraints occur at high currents during passive mode operation due to the large electrode thickness. The variation of Pt loading at the anode or cathode produced an increase of performance compared to the MEA based on 1.5mg cm^{-2} Pt loading on both compartments, but a decrease with respect to the MEA based on 4mg cm^{-2} Pt on both anodes and cathodes. This means that both electrochemical processes appear to limit the stack performance under passive mode operation. Thus, 4mg cm^{-2} Pt loading for both electrodes was selected for further investigations as the best compromise between electrode thickness and amount of catalytic sites.

A maximum power of 225mW (Fig. 4.5b) was obtained at ambient temperature for the three-cell stack (design A) with 4mg cm^{-2} Pt loading on each electrode using 5M methanol concentration at the anode, corresponding to a power density of about 20mW cm^{-2}.

The two stack designs (A and B) were investigated in terms of polarization behavior, output power, electrical resistance and durability with 2 and 5M methanol solutions. Fig. 4.6 shows the polarization and power curves for the two stack designs fed with a methanol concentration of 2M. An OCV of about 2.1V was recorded with the design A; whereas, it was about 1.9V with the type B. Such a higher OCV value recorded for the configuration A with respect to B could be attributed to a lower methanol crossover. Indeed, the presence of the holed mesh in the design A could obstacle or retard methanol permeation through the electrodes and, thus, through the membrane [11], as

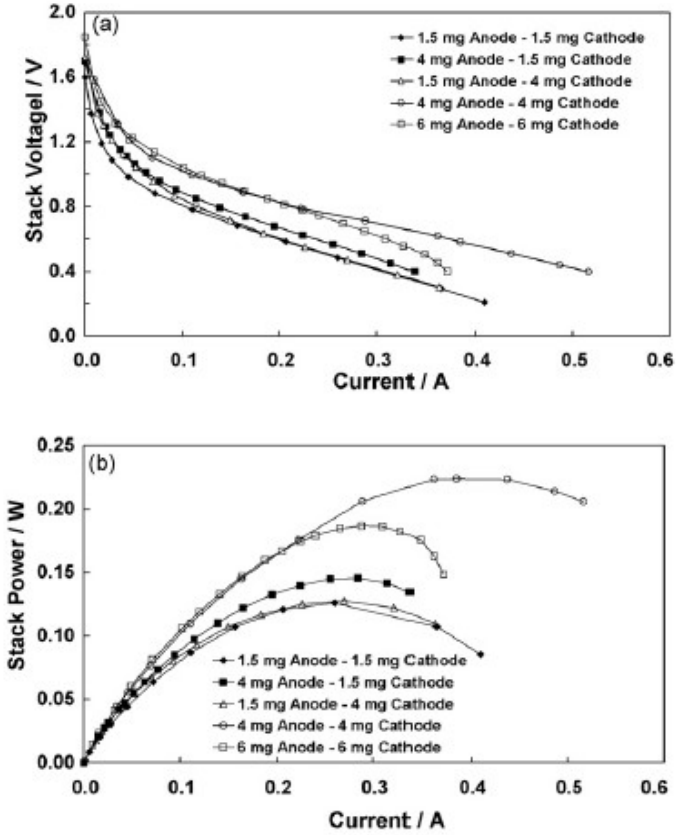

Fig. 4.5: Comparison of the polarization (a) and power (b) curves for the design A stack under different Pt loading at the anodes and cathodes and using 5M methanol solution.

a consequence of a barrier effect similar to that observed when the electrode thickness is increased. This explains also the higher mass transfer constraints of the design A compared to the design B, resulting in a lower output current (Fig. 4.6a) at low voltage. It is derived that, under this configuration, the process is controlled by methanol transport at high currents (460mA at 0.4 V). Whereas, by using design B, no significant diffusion limitation was observed. In the latter case, the obtained maximum current was 550mA at 0.4 V. Furthermore, lower voltage losses for the design A, in the activation region of the polarization curve, are attributed to the lower methanol cross-over compared to design B, in which the anodes are in direct contact with the methanol solution (Figs. 4.2 and 4.3b). However, the maximum power was almost the same for the two configurations, i.e. about 230mW, but it was reached at different stack voltages, 0.6 and 0.5V for the designs A and B, respectively.

A higher efficiency was, accordingly obtained for the design A due to the presence of the holed mesh in the flow fields/current collectors that gave rise to a lower methanol crossover (lower activation polarization); nevertheless, at high currents such a flow field caused a loss in performance due to mass transfer limitations.

The same comparison between the two stack designs was carried out by using a 5M methanol solution at the anode. Fig. 4.7 shows the polarization and power curves for the two stack designs under this condition. A behavior similar to that

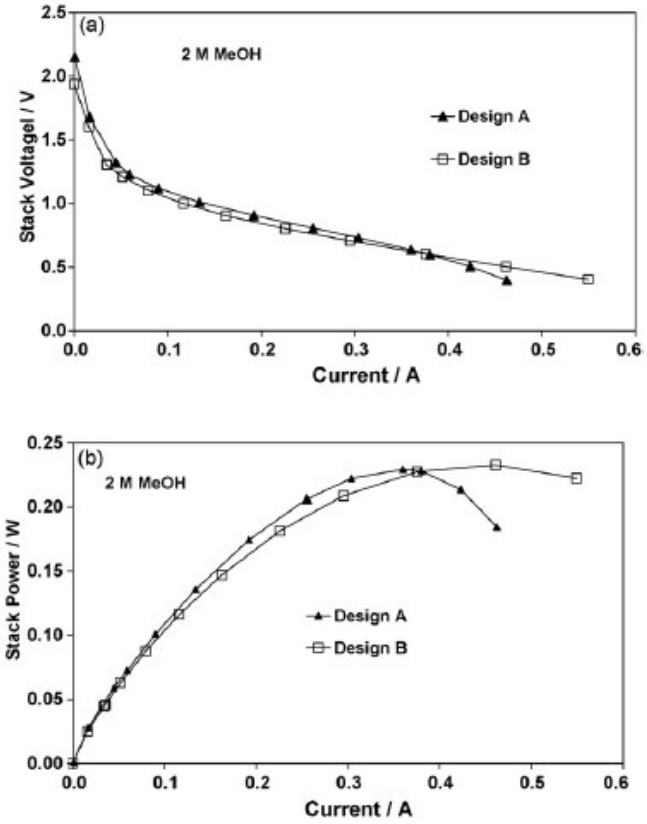

Fig. 4.6: Comparison of the polarization (a) and power (b) curves for the designs A and B using a Pt loading of 4mg cm^{-2} at the anodes and cathodes and 2Mmethanol solution.

recorded in the previous experiment with 2M methanol solution was observed. Yet, the OCV value for both designs is lower in this case due to the larger methanol concentration that produces a larger methanol cross-over, as expected. Also under these conditions, in the mass transport region, the design A shows higher mass transfer polarizations with respect to design B, due to the presence of the small holes (about 1.5mm of diameter) that limit the methanol and oxygen (from ambient air) permeation into the anodes and cathodes, respectively. Also the CO_2 removal from these small holes at the anode could cause an increase of mass transfer limitations. This effect is due to the simultaneous presence of CO_2 bubbles exiting from the holes and methanol solution entering into the holes and diffusing towards the electrodes. The increase of methanol concentration produces an increase of the obtained maximum current for both designs (about 50mA at 0.4 V).

No gain, in terms of output power, was recorded with design A (~230mW); whereas, for design B the maximum power increased of about 10% passing from 2 to 5M of MeOH concentration (~250mW).

The ohmic resistance for both designs was evaluated by means of Electrochemical Impedance Spectroscopy (EIS) at the open circuit potential (OCV). Fig. 4.8 shows the EIS spectra for both configurations. The impedance plots (Nyquist) in Fig. 4.8 show similar series resistance values (high frequency intercept on the real axis) for both systems. This indicates that there are no constraints in terms of electrical contact for the design B as

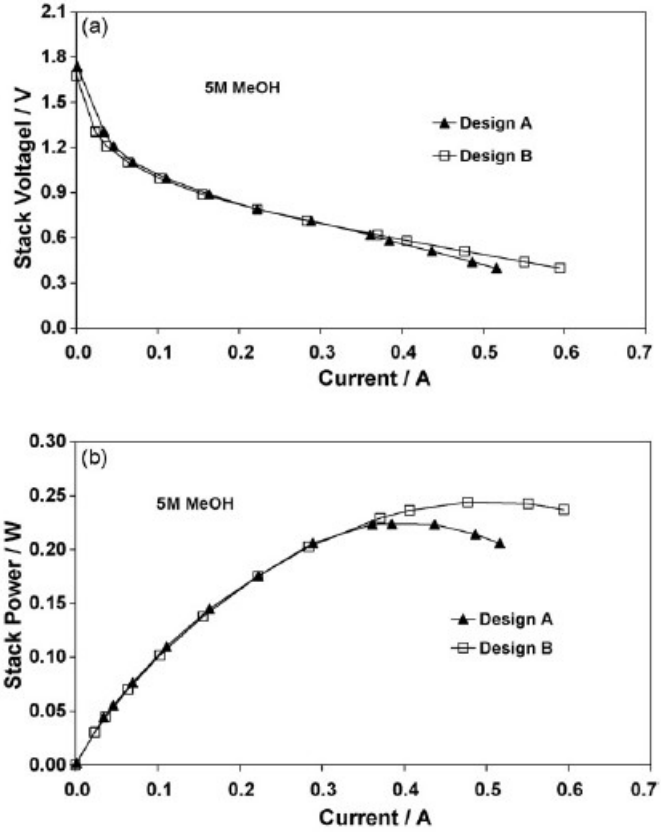

Fig. 4.7: Comparison of the polarization (a) and power (b) curves for the designs A and B using a Pt loading of 4mg cm^{-2} at the anodes and cathodes and 5Mmethanol solution.

compared to design A. As above pointed out, in the design B, the electrical contact with the current collector occurs only at the electrode borders (Figs. 4.2-4.3). No low frequency intercept on the real axis is recorded in Fig. 4.8 in the investigated range of frequencies (105–1 Hz). The slow reaction kinetics in the activation region determine large charge transfer resistance and high relaxation times for the electrochemical process. Furthermore, the data scattering at very low frequency for this device precludes a clear evaluation of the AC-impedance data (not shown). A comparison of the total impedance at low frequency (1 Hz) shows values of 2Ω compared to 1.6Ω for the design A versus the design B. The low frequency impedance values are mainly determined by the activation control being this predominant at high potentials versus ohmic characteristics.

The electrodes are the same in both devices; yet, possibly due to the different methanol poisoning effect caused by the cross-over at the cathode, the design A is more performing in the activation region than the design B. At intermediate frequencies, the capacitance [$C = 1/(2\pi fZ'')$] is larger for the design B. This difference can be explained by considering that the different designs may change the wetting behavior of the electrodes and thus the pores filling properties. These effects influence the capacitive characteristics. The wetting properties contribute to determine the better performance of the design B versus A at high current densities (Fig. 4.7). Fig. 4.9 shows a time-stability test carried out at 250mA on both stack

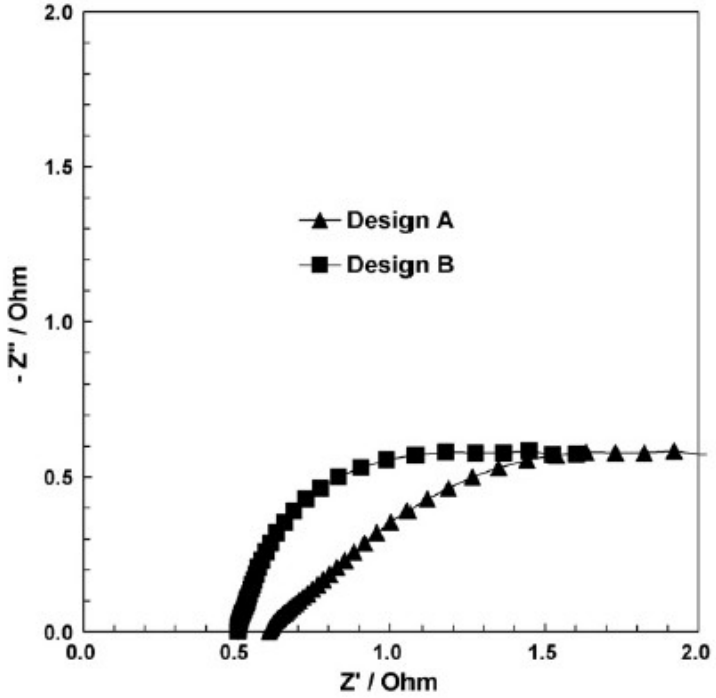

Fig. 4.8: Impedance spectra of the two designs at OCV, using 5M methanol solution.

configurations. The reservoirs were filled with 21 ml of 5M methanol solution for both designs. Also a theoretical chrono-potentiometric curve, based on the theoretical fuel efficiency and assuming the same initial over-potential, is reported in the figure for comparison. A different behavior as a function of the adopted design was observed. For the type A, a rapid decrease of performance was recorded after about 5 h of operation. Lai et al. [14] attributed this effect to a large amount of water that was produced at these currents at the cathode, therefore causing a flooding of electrodes and blocking the air path. In agreement with Lai et al. [14], we can think that the presence of small holes for the design A makes more difficult to remove the water from the cathode; accordingly, it is difficult for oxygen to reach the flooded cathode reaction region. This effect is less significant for the design B due to the large interface between the electrodes and ambient air.

Furthermore, such a decrease of performance with time for design A could be also partially attributed to the CO_2 removal from the holed mesh at the anode. Indeed, if methanol solution in the reservoir of stack A was stirred after the voltage drop, the performance increased up to reach the initial value. Unfortunately, after short time a similar voltage loss was observed again. In fact, after a few hours of continuous operation for the stack A all the holes seemed to be covered by CO_2 bubbles that hindered the methanol solution to reach the catalytic sites. This produced the rapid decrease of voltage. Such an effect was not observed for the design B, where an easy removal of CO_2 was produced by the extension of the

interface between the electrodes and the reservoir, easing methanol access to the reaction area. This allowed to reach 17 h of continuous operation, with only a slight decrease of performance with time. A drastic voltage loss was observed

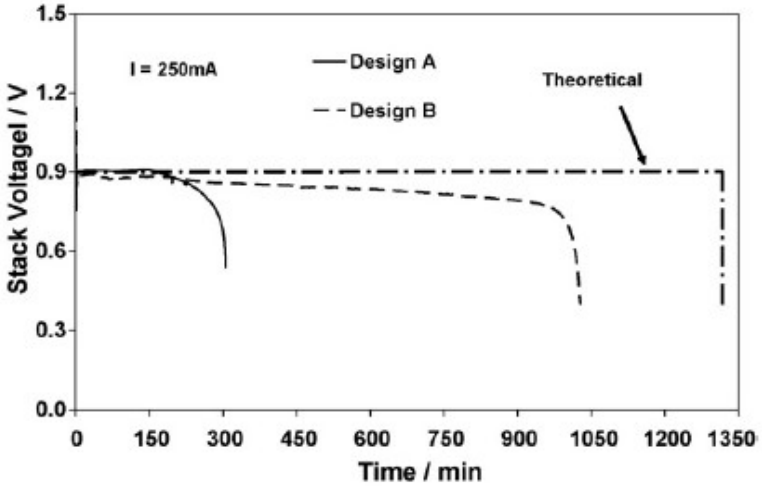

Fig. 4.9: Chrono-potentiometric results at 250mA obtained with the two designs using a Pt loading of 4mg cm^{-2} on each electrode and 5M methanol solution. The difference between design A and B are due mainly to the CO_2 entrapment within the mesh in design A. The difference between design B and theoretical curve is mainly due to fuel cross-over through the electrolyte.

when the methanol concentration in the reservoir was less than 0.1M. Obviously, with a single charge of methanol solution, the maximum operation time was less than the theoretical value (about 22 h) because of the methanol cross-over through the membrane reducing the reactant content at the anode compartment.

It has been evaluated the methanol crossover rate for both designs on the basis of the Faradaic efficiency determination (fuel efficiency) when all methanol in the tank was consumed (before re-fueling). Usually, the methanol cross-over is determined by measuring the CO_2 content in the outlet cathode stream by an Infrared detector while cell is under operation [16]. The liquid fraction in the cathode stream is first condensed at low temperature, whereas the gas escaping from the condenser is further purified by passing it through a magnesium perchlorate bed before being analyzed by the infrared sensor [16]. Yet, due to the fact that no air flow at the cathode is used, the CO_2 sensor method is not applicable in the present case. Alternatively, electrochemical determination of methanol passed at the cathode by measuring the methanol oxidation current at the cathode in the presence of an inert gas [17] does not appear appropriate. This method discards the effects of operating current density (concentration gradient at the anode–electrolyte interface) and electro-osmotic drag. Our approach is based on the assumption that the reduction of Faradaic efficiency from the ideal 100% is only due to the methanol loss by the cross-over through the membrane. The chromatographic analysis of the methanol solution in the tank

showed no organic compounds other than methanol and CO_2 at the anode compartment during operation [18]. Particular care was addressed to reduce any methanol loss from the tank by evaporation, and the methanol solution in the design A was mechanically stirred after each potential drop. The reproducibility in the measurement of methanol cross-over was determined by repeating the experiments four times. The average value with the deviation observed in the different experiments is reported below. From this analysis, a total methanol cross-over rate of $1.5\pm0.2\times10^{-6}$ and $1.8\pm0.2\times10^{-6}$ mol min^{-1} cm^{-2} in the stacks A and B, respectively, at 21 °C was determined under passive mode operation with 5M MeOH, 4mg Pt loading on both electrodes and 250mA operating current. Accordingly, the fuel efficiency was 81.2% for the design A and 78.2% for the design B. But, the design A requires to be mechanically agitated to reach this efficiency level.

4.4. Conclusions

The comparison between two designs of flow fields/current collectors for a passive DMFC monopolar three cell stack has evidenced the better performances of the design B, which features a peripheral frame current collector and open area at anode and cathode inlets). Performance and discharge behavior have been investigated under several different conditions in terms of catalyst load and fuel concentration for design A and

then the best configuration has been used to compare design A and B. Similar performances in terms of maximum power were recorded; whereas, better mass transport characteristics were obtained with the design B. To the opposite, OCV and stack voltages at low current were sensibly higher using design A as a consequence of lower methanol cross-over. Longer time-operation (17 h) with a unique MeOH charge and no external aid was recorded with design B compared to A (5 h), mainly due to an easier CO_2 removal from the stack, which ease the fuel access to the anode in design A.

4.5. References

1. G.Q. Lu, C.Y.Wang, T.J. Yen, X. Zhang, Electrochim. Acta 49 (2004) 821.
2. G. D'Arrigo, C. Spinella, G. Arena, S. Lorenti, Fuel Cells Bull. 4 (2003) 10.
3. J. Bostaph, R. Koripella, A. Fisher,D. Zindel, J. Hallmark, Proceedings of the 199th Meeting on Direct Methanol Fuel Cells Electrochemical Society, Washington D.C., USA, 25–29 March 2001, 2001.
4. G. Jewett, Z. Guo, A. Faghri, J. Power Sources 168 (2007) 434.
5. R. Chen, T.S. Zhao, J. Power Sources 167 (2007) 455.
6. J.J. Martin,W. Qian, H.Wang, V. Neburchilov, J. Zhang, D.P.Wilkinson, Z. Chang, J. Power Sources 164 (2007) 287.
7. R. Chen, T.S. Zhao, Electrochim. Acta 52 (2007) 4317.
8. R. Chen, T.S. Zhao, Electrochem. Commun. 9 (2007) 718.
9. M.A. Abdelkareem, N. Nakagawa, J. Power Sources 165 (2007) 685.
10. Z. Guo, A. Faghri, J. Power Sources 160 (2006) 1183.
11. Y.H. Pan, J. Power Sources 161 (2006) 282.
12. H. Chang, J.R. Kim, J.H. Cho, H.K. Kim, K.H. Choi, Solid State Ionics 148 (2002) 601.
13. M.S. Yazici, J. Power Sources 166 (2007) 137.

14. Q.-Z. Lai, G.-P. Yin, J. Zhang, Z.-B. Wang, K.-D. Cai, P. Liu, J. Power Sources 175 (2008) 458.

15. V. Baglio, A. Di Blasi, E. Modica, P. Cretì, V. Antonucci, A.S. Aricò, J. New Mater. Electrochem. Syst. 9 (2006) 41.

16. A.S. Aricò, V. Baglio, P. Cretì, A. Di Blasi, V. Antonucci, J. Brunea, A. Chapotot, A. Bozzi, J. Schoemans, J. Power Sources 123 (2003) 107.

17. F. Liu, G. Lu, C.-Y.Wang, J. Electrochem. Soc. 153 (2006) A543.

18. A. Oedegaard, J. Power Sources 157 (2006) 244.

5. Impedance measurement and testing

5.1. Design review

The simple design of a planar three cell stack operating in passive mode has been tested under different fuel concentration and catalyst load in chapter 3. Due to passive mode operation, performance are not comparable to those of more complex systems operating at high temperature (130°C) and with the assistance of auxiliaries (pumps, fans etc.), but its simplicity makes this system a viable solution for portable applications. It is simple to manufacture, reliable, cheap and virtually maintenance-less. Some design issues have been faced and partially solved by removing the holed mesh area of design A and leaving the electrode area exposed to ambient air and fuel. Excessive membrane swelling, typical of very concentrated methanol-water mixture, results sometimes in a loss of contact between the the electrode and the current collector (that in the design B is reduced to a frame around the electrode) or in some leakage. Both issues can be recovered by reassembling the stack but still require a maintenance operation. The issues related to CO_2 bubble formation in the first design have been solved, achieving optimal performances in terms of fuel utilization and operation time.

Fuel crossover is still an unsolved issue, because mainly related to membrane. Actual Nafion®-based electrolytes, although representing the established standard, feature a large crossover when dealing with liquid methanol in DMFC. Other polymers, such as those commercialized by Polyfuel, seem to attract manufacture's attention but, unfortunately, not much is currently available in literature, except Polyfuel's data sheets*.

5.2. Electrode design and testing

The quest for better stack performances, in terms of cross-over mitigation, requires an investigation of electrode influence and properties. The hydrophobic properties of the electrode structure influence significantly the water migration within the electrode. It works also with the water-methanol used as fuel, hence crossover can be managed by increasing the hydrophobicity of the electrode. In the present chapter there are investigated different membrane-electrode assemblies (MEAs) characterized by different hydrophobic–hydrophilic properties in a passive direct methanol fuel cell (DMFC) monopolar mini-stack at room temperature. These properties were modulated by varying the amount of Nafion or replacing the ionomer in the catalytic layer with polytetrafluoroethylene (PTFE). Impedance

* At the time of revising this work, Polyfuel's web site (www.polyfuel.com) was down due to a massive hacker attack and the domain was temporarily banned.

spectroscopy provided valuable information with respect to the limiting processes occurring during fuel cell operation. Methanol crossover, especially in the presence of high methanol concentration, played a major role in determining the overall performance. The development of a methanol-impermeable membrane appears crucial to increase the performance of DMFC devices for portable applications.

Significant efforts are presently dedicated to develop new concepts of DMFC stacks [17-18, 21–24] in order to miniaturize the device; yet, less attention is focused on the optimization of electrode structures for a suitable mass transport of reactants and to foster methanol tolerance at the cathode in a passive mode stack [25–27]. High Pt loadings (4 mg cm^{-2}) are currently necessary for the methanol electro-oxidation reaction and oxygen reduction reaction to proceed at acceptable rates in passive mode DMFC devices. There are various limitations in the use of catalyst layers of large thickness in these systems; i.e. it reduces the electro-catalyst utilization and causes an increase in ohmic and mass-transport polarisations; these aspects have suggested the use of unsupported electro-catalysts. These catalysts are currently used as anode and cathode catalysts in DMFCs operating at low temperatures (20–60 °C) for portable applications [7, 11, 14, 24].

Actually, DMFC electrodes are derived from gas diffusion electrodes, similar to those used in H_2-fueled proton exchange fuel cells (PEFCs) [28–31]. The typical configuration feature a

macroporous layer, made of a carbon -cloth or -paper; this is the conductive support where the microporous gas diffusion layer and the catalytic layer are deposited. In most electrode configurations, the gas diffusion layer is composed of Poly(tetrafluoroetylene) (PTFE) and carbon black, whereas the composite catalytic layer consists of carbon supported Pt or Pt alloy catalysts and Nafion ionomer. Such an electrode structure was originally developed for operation at about 80 °C, since the development of DMFCs for transportation was historically considered for large-scale application of such devices [1-4]. In low temperature liquid-fueled DMFCs for portable systems, beside the poor electrocatalytic activity at low temperatures, this electrode configuration suffers of mass-transport limitations. These constraints mainly occur at the anode side due to the low diffusion coefficient of methanol in water and the release of carbon dioxide gas bubbles [5, 32].

Some recent studies have been addressed to replace the carbon cloth or carbon paper support with a titanium net [32] to enhance mass transport. DMFCs are generally operated with aqueous methanol solution at different concentrations; therefore, in order to ensure a better reactant distribution and supply, good hydrophilicity is required for the anode side, whereas, at the cathode, hydrophobic properties are required to avoid electrode flooding, especially under low temperature operation using a high methanol concentration at the anode.

5.3. Electrode characterization

The effect of MEA configuration on the behavior of a monopolar mini-stack operating at ambient temperature can be evaluated, under conditions close to the practical application (high methanol concentration at the anode, passive mode, air breathing) by impedance measurements. This research is not addressed to the optimization of the MEA configuration, to achieve the best performance for the DMFC device, but to qualify the relevant phenomena occurring under passive mode operation. To achieve this target, distinct electrode properties were selected in order to associate the response of the electrochemical diagnostics to the characteristics of the MEA structure.

The hardware used to test and qualify the MEAs is the same monopolar three-cell stack already evaluated in previous chapters, featured by consisted of two polymeric plates (printed circuit boards – PCBs) without any specific flow field for liquid/gas diffusion [33]; a thin gold film, deposited on the external borders of the fuel and oxidant compartment apertures, act as the current collectors where the electrodes were placed in contact (Figure 1). In this design, the central part of the electrode is exposed directly to the ambient air (for the cathodes) and methanol solution (for the anodes). The two plates were assembled as shown in Figure 5.1. This design was selected due to its simplicity; moreover, no significant ohmic drop was measured within current collectors/ external circuit.

The geometrical area of each electrode was 4 cm^2 and the total area of the stack was 12 cm^2. A methanol reservoir (containing in total 21ml of methanol solution, divided into three compartments), with three small holes in the upper part to fill the containers and to release the produced CO_2, was attached to

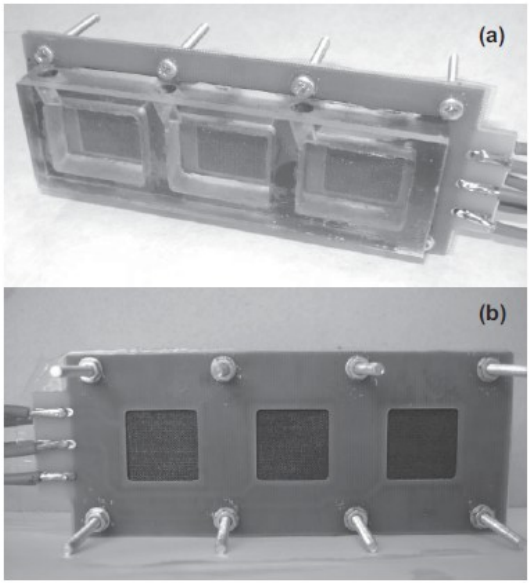

Fig. 5.1: the three cell planar stack used for testing different MEAs. In (a) it is visible the fuel compartment and the anode side. In (b) the cathodes.

the anode side. The MEAs for this stack design (3 cells) were manufactured by simultaneously assembling three sets of anode and cathode pairs on each side of the membrane and then sandwiched between the two PCBs. Series connections between the cells were made externally through the electric circuit. The MEA design in this monopolar stack is not significantly different from that of a single cell. Thus, the approach is useful for fundamental investigations under conditions appropriate for the application in portable electronic devices. The standard electrodes used in our previous works [33, 34] consisted of composite catalytic layers with 15 wt.-% ionomer and 85 wt.% catalyst, and commercial backing layers HT-type (E-TEK) at the anode and LT-type (E-TEK) at the cathode.

Three different MEA configurations were prepared, assembled and investigated (MEA 1, MEA 2 and MEA 3). An unsupported Pt-Ru (Johnson-Matthey) was used as the anode catalyst and a Pt black (Johnson-Matthey) catalyst was utilized at the cathode for all MEAs. For MEA 1, the anode catalyst was mixed with 5 wt.-% Nafion ionomer (Ion Power, 5 wt.-% solution) and deposited onto the backing layer, composed of carbon cloth, acetylene black and 10 wt.% Nafion in order to make the electrode hydrophilic [34]. The cathode catalyst was mixed with 15 wt.% Nafion ionomer (Ion Power, 5 wt.% solution) for the MEA 1 and deposited onto a commercial LT-ELAT (ETEK) backing layer. For the MEA 2, the anode catalyst was mixed with 15 wt.-% Nafion ionomer (Ion Power, 5 wt.-% solution) and deposited onto a commercial HT-ELAT (E-TEK) backing

layer. The cathode catalyst for MEA 2 was mixed with 30 wt.% PTFE in order to make the catalytic layer hydrophobic. This paste was spread onto a commercial LT-ELAT (E-TEK) support. The complete electrode in the latter case was sintered at 350 °C for 30 min in an oven. For MEA 3, the anode was the same as that used for the fabrication of MEA 2. The cathode was the same as that used in MEA 1. Such a configuration was already investigated only in terms of performance in a previous paper [33].

Summarising MEAs properties, MEA 1 featured a hydrophilic anode and standard cathode, MEA 2 featured a standard anode and hydrophobic cathode and MEA 3 was provided with a standard anode and standard cathode.

A Pt loading of 4 mg cm^{-2} was used for all MEAs, both at the anode and cathode. Nafion 117 (Ion Power) was used as electrolyte. The stack was operating under passive mode at room temperature (21±2°C). Different methanol concentrations (from 1 to 17M) were used. Performances were investigated by steady-state galvanostatic polarisations by using an AUTOLAB PGSTAT 302 Potentiostat/Galvanostat (Metrohm) equipped with a FRA. The polarisation curves were recorded just after filling the reservoir with the methanol solution, in order to limit the increase of temperature due to methanol crossover [35, 36]. The impedance measurements were performed in a frequency range between 1 MHz and 0.01 Hz by frequency sweeping in the single sine mode. Also in this case, the experiments were carried out in order to maintain the temperature similar for all

measurements. This was obtained by cooling down the stack after each measurement and changing the methanol solution. In-situ methanol crossover was determined by measuring the CO_2 concentration close to the cathode backing layer after subtraction of the background CO_2 level measured by a calibrated CO_2 sensor.

5.4. Experimental results and evaluation

The limiting processes under different operating conditions and for different MEA configurations have been evaluated by means of impedance measurements. This has been done by varying methanol concentration at the anode and the oxidant at the cathode. Table 5.1 summarizes the characteristics of the different MEAs.

In the MEA 1, the anode was prepared differently from that reported in a previous experiment [33]; in fact, the presence of Nafion instead of PTFE in the diffusion layer ensures an increased hydrophilic character to the electrode backing. Furthermore, a lower amount of Nafion in the catalytic layer was used to enhance the mass transfer properties in the active region [34]. MEA 1 was first characterized electrochemically by polarization and impedance measurements at different methanol concentrations (from 1 to 10 M). Figure 5.2 shows the polarization curves recorded for the MEA 1 at different methanol concentrations in the passive mode. The open circuit potential (OCV) for the stack decreased as the methanol

concentration increased; this clearly indicates an increase in methanol crossover rate with an increase in methanol concentration. It is evident that the performance recorded with 1 M methanol solution is better than that obtained with higher concentrations. This means that the presence of a hydrophilic anode enhances methanol transport, also in the presence of a low methanol concentration, but, it simultaneously enhances methanol crossover. No barrier effect for MeOH permeation is produced by this electrode configuration. In fact, the OCV was quite low compared to our previous investigations [33, 37]. By increasing the methanol concentration, the OCV and the performance are, in the present case, lower than those obtained with 1 M solution in the whole range of current. This is due to the permeation of methanol to the cathode through the Nafion membrane, whose swelling increases with the increase in

		MEA 1	MEA 2	MEA 3
Anode	Diffusion layer	90% carbon 10% Nafion	HT-ELAT (E-TEK)	HT-ELAT (E-TEK)
	Catalytic layer	95% catalyst 5% Nafion	85% catalyst 15% Nafion	85% catalyst 15% Nafion
Cathode	Diffusion layer	LT-ELAT (E-TEK)	LT-ELAT (E-TEK)	LT-ELAT (E-TEK)
	Catalytic layer	85% catalyst 15% Nafion	70% catalyst 30% PTFE	85% catalyst 15% Nafion

Table 5.1: main features of the tested electrode set

methanol concentration [38]. Moreover, passing from 2 to 5 M, the OCV and potential at low current density decreases as expected due to a higher methanol crossover.

At lower potential, a higher methanol concentration produces an increase in current density due to a larger methanol availability that reduces the mass transfer polarization. By further increasing the methanol concentration (10 M), the performance decreases due to the large swelling of the membrane that produces a higher methanol crossover. There is a significantly lower OCV due to the increased crossover with

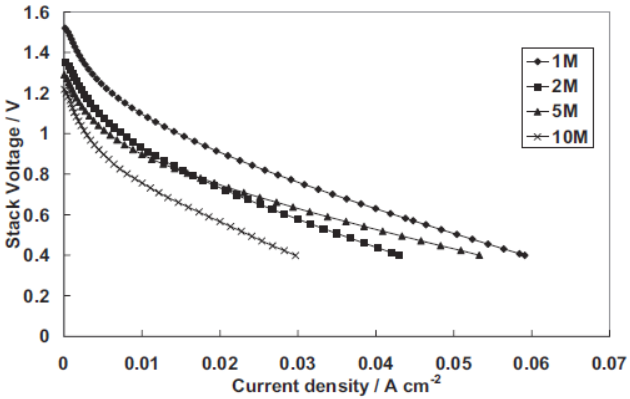

Fig. 5.2: polarization curves at different fuel concentrations for MEA 1

10 M concentration; the voltage loss in this case is reflected in the overall polarization curve. The presence of methanol at the cathode produces a mixed potential that reduces the voltage of the stack. In such a system, where the performance is governed by a number of coupled processes proceeding at different rates, impedance spectroscopy becomes a common tool in the characterization [39–41]. Thus, impedance spectra were recorded with MEA 1 at different cell voltages, 0.4, 0.7, 1.1 and OCV, and different methanol concentrations, (a) 1 M, (b) 5 M and (c) 10 M. They are reported in Figure 5.3 in the Nyquist form. They consist of two strongly overlapping semicircles, a small one at high frequency and a large one at low frequency. At the OCV, the charge transfer resistance for the whole process is the largest and it decreases by lowering the potential, as expected. Increasing methanol concentration and decreasing cell voltage, an inductive loop is observed at low frequencies.

This inductive loop is quite evident in the presence of 10 M methanol; however, it is also visible, even if less evident, at lower methanol concentrations. The inductive loop appears enhanced by the permeation of methanol to the cathode side. In order to confirm this hypothesis and evaluate where the semicircle at low frequency is related to the cathodic process, the operation mode at the cathode compartment was only switched from passive (air breathing) to active, by flowing pure oxygen over the stack cathode backings.

The impedance spectra recorded in the presence of static air, an oxygen flow at the cathode and different methanol concentrations at the anode are reported in Figure 5.4. This approach facilitates the identification of the process associated with the low frequency semicircle. A strong variation in the charge transfer resistance passing from oxygen to static air is observed. The low frequency semicircle is significantly larger in the presence of air than in the presence of oxygen at two different stack voltages using 10 M methanol at the anode (Figure 5.4a, b), whereas the two plots are similar in the

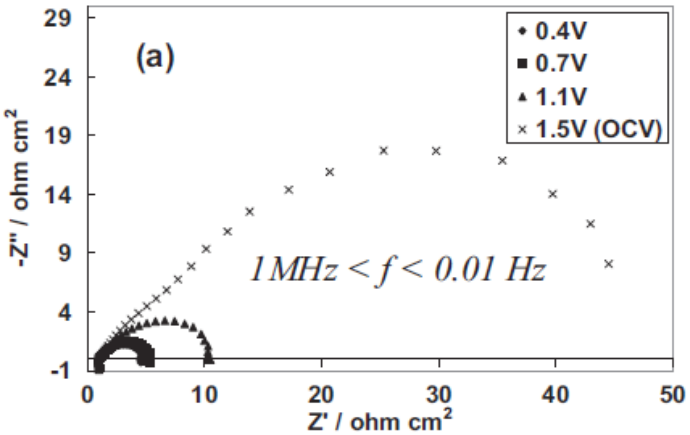

Fig. 5.3 (a): impedance spectrum at different cell voltage and 1 M.

presence of 2 M methanol (Figure 5.4c). This indicates that at high methanol concentration the limiting process is concerned with the cathode operation due to the strong methanol crossover. In fact, when oxygen is used, the semicircle at low frequency is smaller than that with air. Such evidence suggests that a high oxygen partial pressure can mitigate the poisoning effect of methanol at the cathode.

An inductive loop at low frequency was already observed in the ac-impedance spectra carried out in the half-cell for the

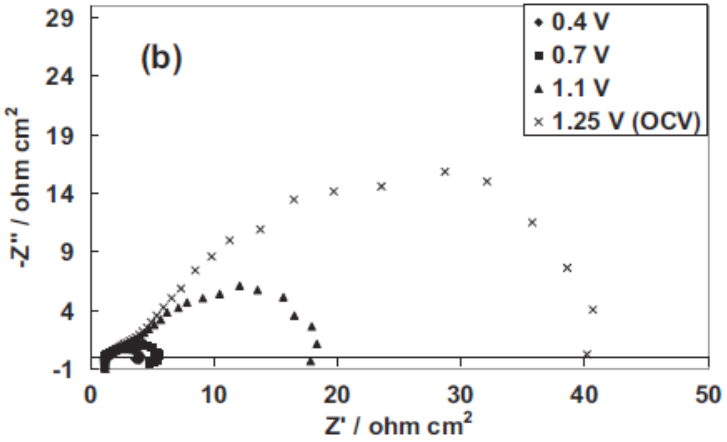

Fig. 5.3 (b): impedance spectrum at different cell voltage and 5 M.

oxygen reduction at porous gas diffusion electrodes in a liquid electrolyte [42]. These features are usually attributed to adsorption–desorption phenomena occurring in heterogeneous reactions [42–45]. The inductive loop observed for the oxygen reduction in a liquid electrolyte half-cell was especially occurring at high potentials. It was, thus, related to the presence of O-ads and OH-ads species as stable intermediates in the reaction pathway of oxygen reduction [45]. In this case, the inductive loops are more evident at low cell voltages (see Figure 5.3) corresponding to low cathode voltages. This evidence is certainly related to the effect of methanol adsorption on the cathode due to the crossover, which is more

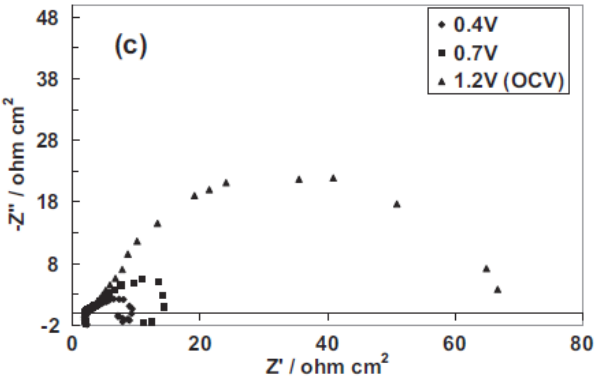

Fig. 5.3 (c): impedance spectrum at different cell voltage and 10 M.

effective at low cathode potentials, whereas at high potentials methanol is oxidized quickly to CO_2.

A CO_2 sensor used for environmental analysis purposes was allocated close to cathode backings and the steady-state CO_2 concentration was measured and subtracted to the CO_2 background from the laboratory environment. The background level of CO_2 was measured at a reasonable distance from the fuel cell test station. This approach was used to evaluate the amount of methanol permeation under specific conditions of

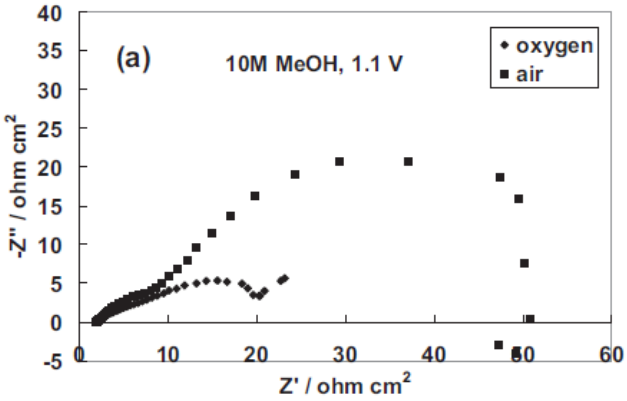

Fig. 5.4 (a): Effect of oxidant on the impedance spectra for MEA 1 at 1.1 V and 10 M methanol concentration. Frequency range between 1 MHz and 0.01 Hz.

operating current and methanol concentration for the different MEA configurations.

For MEA 1 the methanol crossover rate was about 3.1 ± 0.2 × 10^{-6} mol min^{-1} cm^{-2}, when a 5 M methanol solution was fed at the anode and the cell was operated at 100 mA.

In MEA 2 the cathode structure was modified by the introduction of PTFE (30 wt.%) instead of Nafion (15 wt.%) in order to increase the hydrophobic properties of the catalytic layer reducing, thus, the wettability of the cathode and

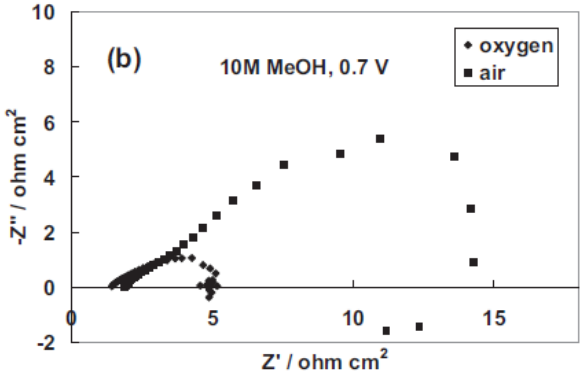

Fig. 5.4 (b): Effect of oxidant on the impedance spectra for MEA 1 at 0,7 V and 10 M methanol concentration. Frequency range between 1 MHz and 0.01 Hz.

consequently the poisoning effect of methanol. A standard anode was used (see experimental part). This anode was characterized by a lower hydrophilicity compared to MEA 1. This approach should reduce the rate of methanol transport through the electrode/electrolyte interface. This MEA 2 was investigated in the monopolar stack under passive mode operation only. The polarization curves at different methanol concentrations are shown in Figure 5.5. An OCV higher than that recorded with MEA 1 was observed, indicating either a reduced methanol crossover or a higher tolerance of the cathode to the methanol passed through the membrane. Also in

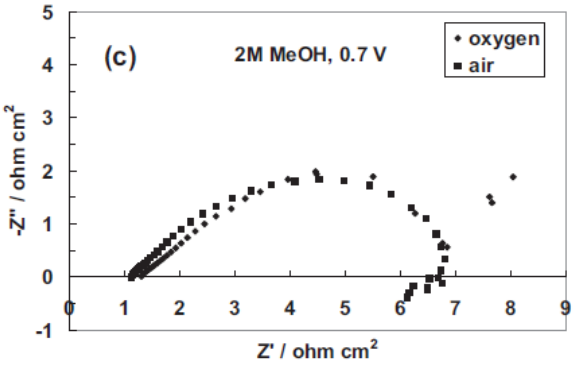

Fig. 5.4 (c): Effect of oxidant on the impedance spectra for MEA 1 at 0,7 V and 2 M methanol concentration. Frequency range between 1 MHz and 0.01 Hz.

this case, as expected, there is a decrease in OCV as the methanol concentration increases; yet, the overall performance is lower than that recorded for MEA 1 at the different methanol concentrations, especially at high currents. This is due to the absence of Nafion in the catalytic layer of the cathode that is required to extend the three-phase reaction zone. Thus, due to the fact that the triple-phase boundary is limited to the interface between the catalytic layer and the membrane, the

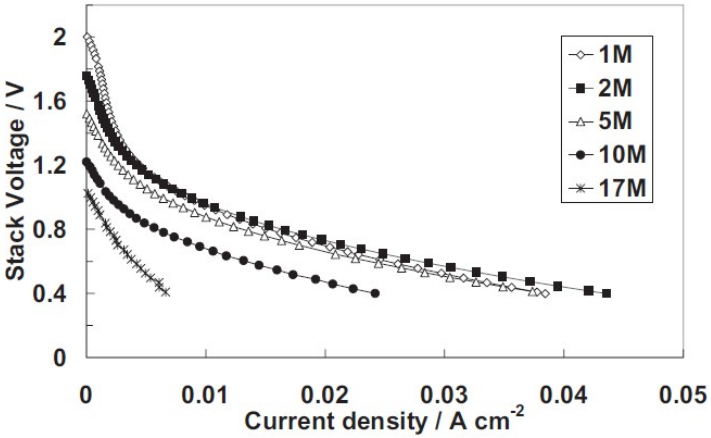

Fig. 5.5: Polarisation curves for MEA 2 at different methanol concentrations.

electrochemical active surface area should be lower for the cathode in MEA 2 with respect to MEA 1.

The performance is affected by this decrease in the active catalytic sites and also by the increase in the electrical resistance caused by the presence of a large amount of non-conducting material, i.e. 30 wt.-% PTFE, in the cathode active layer. However, the large cathode hydrophobicity allowed a proper investigation of the stack behavior in the presence of large methanol concentration. A methanol/water solution with a molar ratio 1:1 (17 M methanol solution), corresponding to the stoichiometry of the anode reaction, was fed at the anode compartment. The polarization plot is reported in Figure 5.5 and shows an OCV slightly higher than 1 V for the stack and a dramatic loss of potential as the current increases. This effect was caused by a strong increase in the methanol crossover. Impedance spectra, recorded for MEA 2 fed with 5 M methanol solution at different voltages, are reported in Figure 5.6. A different profile was observed compared to the spectra obtained for MEA 1. In this case, two comparable semicircles are present at intermediate potentials, e.g. 1.3 V.

At the OCV, the second semicircle is slightly larger than the first one, indicating a large poisoning effect of methanol at the cathode when the circuit is open (no current is flowing, thus no methanol is consumed).The identification of the cathodic process as the limiting one for MEA 1 is confirmed by the comparison of the impedance spectra for MEA 1 and MEA 2 at different voltages with 1 M methanol solution at the anode and

ambient air at the cathode (Figure 5.7). A different behavior is observed for the two MEAs, both at 0.4 and 1.1 V; in fact, in the MEA 1 (hydrophilic cathode) the second semicircle (ascribed to the cathode by previous experiments) is larger than the first one (anode); whereas, for MEA 2 (hydrophobic cathode) two comparable semicircles are present, indicating similar reaction rates for the anodic and cathodic processes.

At high current (stack voltage 0.4 V), the anodic process is the limiting step for MEA 2 (hydrophobic cathode) in the presence

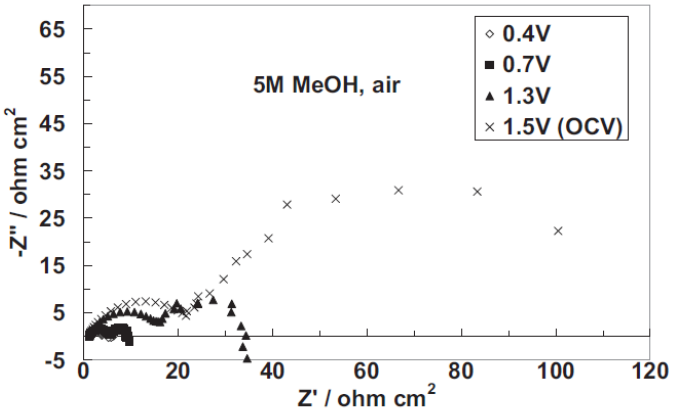

Fig. 5.6: Impedance spectra recorded for MEA 2 with 5 M methanol concentration at different voltages. Frequency range between 1 MHz and 0.01 Hz.

of a low methanol concentration (1 M). The level of methanol crossover was evaluated by the same approach used for the MEA 1 and under the same condition (5 M MeOH at the anode). The observed value was significantly lower ($1.9 \pm 0.2 \times 10^{-6}$ mol min^{-1} cm^{-2}). Due to the low methanol crossover in these conditions the cathode performs suitably. A methanol/water back diffusion process from the hydrophobic cathode to the anode through the membrane may also occur. Thus, this cathodic structure could be promising for operation with high methanol concentration (as requested for commercial applications). Yet, as observed from the polarization curve recorded with 17M methanol solution (Figure 5.5) and from the impedance spectra shown in Figure 5.8, the performance is poor due to the methanol crossover, which also produces, in a few minutes, an increase in temperature with a consequent evaporation of methanol (the liquid solution in the reservoir in contact with the anode was spontaneously boiling under such a condition). Also the impedance spectra in Figure 5.8 are scattered due to the heat released by methanol combustion at the cathode. This strongly suggests the development of proper methanol impermeable membranes. As a comparison, a third MEA (MEA 3), composed of conventional anode (the same used in MEA 2) and cathode (the same of MEA 1), was investigated. The polarization curves are reported in Figure 5.9a. The OCV decreases as the methanol concentration increases, while the limiting current increases with the increase in methanol concentration up to 5 M. In the presence of a 10 M methanol solution, the high methanol crossover produces a

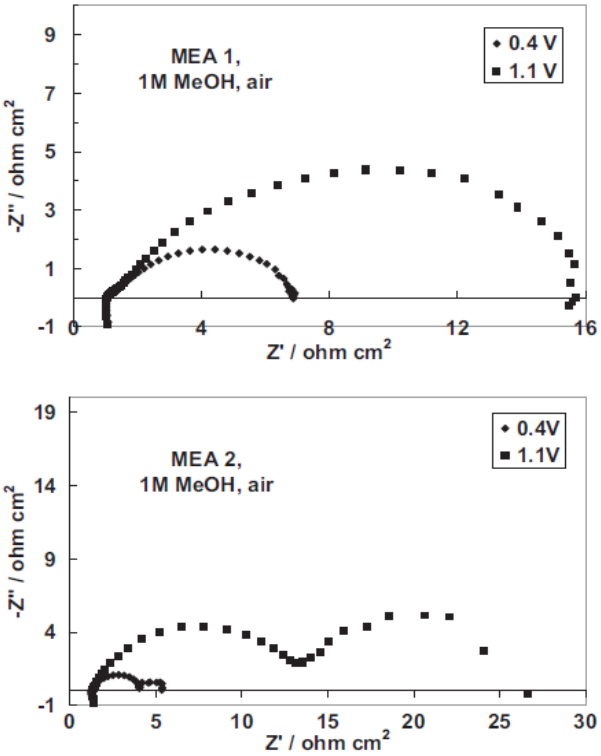

Fig. 5.7 Comparison of the impedance spectra for MEA 1 and MEA 2 at different voltages with 1 M methanol solution at the anode and ambient air at the cathode. Frequency range between 1 MHz and 0.01 Hz.

large loss of potential in the whole polarization curve. The performance with 2M was approaching that of 5M methanol solution. A maximum power of 250 mW was obtained with 5M methanol concentration, corresponding to a power density for each MEA in the stack of about 20 mW cm^{-2} (Figure 5.9b). The methanol crossover rate in this case was $2.0 \pm 0.2 \times 10^{-6}$ mol min^{-1} cm^{-2}, i.e. slightly larger than that recorded for MEA 2 under same conditions (5M, 100 mA of current). Since the

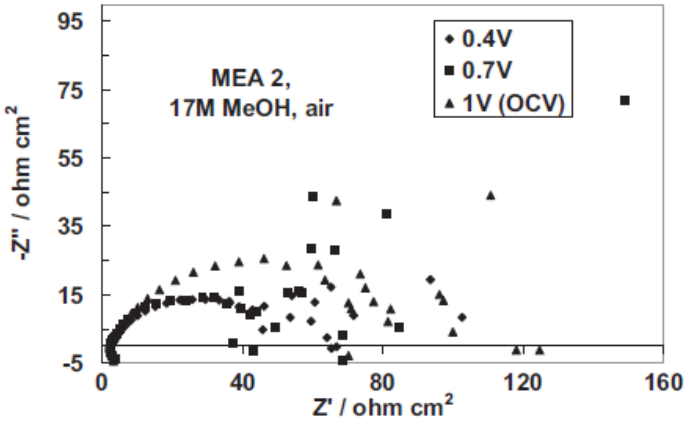

Fig. 5.8 Impedance spectra for MEA 2 recorded at different voltages using 17 M methanol at the anode and ambient air at the cathode. Frequency range between 1 MHz and 0.01 Hz.

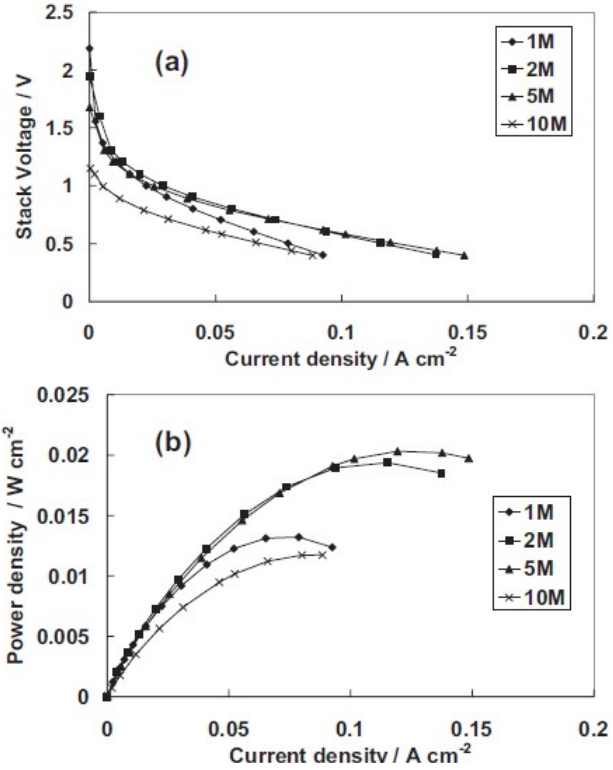

Fig. 5.9 Polarisation (a) and power (b) curves for MEA 3 at different methanol concentrations.

same anode configuration and membrane were used, this small difference could be attributed to the lower affinity to methanol/water of this cathode electrode, causing a small back diffusion. However, the differences between these values of methanol crossover are within the experimental error.

Impedance spectra recorded with MEA 3 in 1 M methanol solution at different voltages are shown in Figure 10. Two comparable semicircles are present at high and low potentials

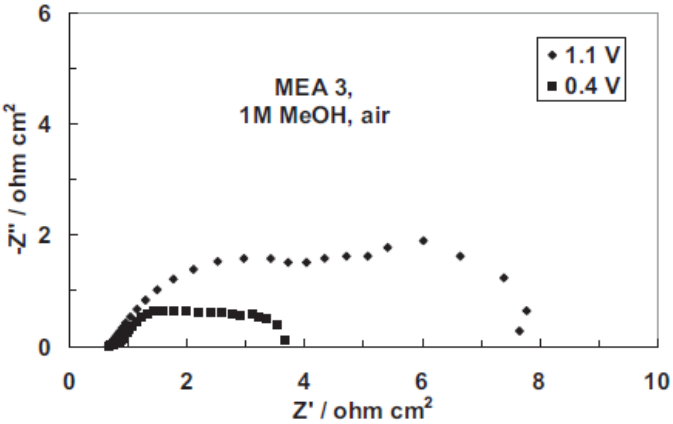

Fig. 5.10 Impedance spectra for MEA 3 recorded at different voltages using 1 M methanol at the anode and ambient air at the cathode. Frequency range between 1 MHz and 0.01 Hz.

as also recorded for MEA 2, but, in this case (MEA 3), a lower charge transfer resistance is shown, indicating a better catalytic behavior (compared to MEA 2) of this MEA. This was attributed to a suitable amount of Nafion in the catalytic layer -1 of the cathode and to a more hydrophobic diffusion layer at the anode (compared to MEA 1). From all these analyzes, it is derived that a proper tailoring of the electrode structure (hydrophobicity/hydrophilicity) is important for passive mode operation.

5.5. Conclusion

The effect of MEA configuration on the performance of a monopolar mini-stack operating at low temperature, under conditions close to the practical application (high methanol concentration at the anode, passive mode, air breathing) was evaluated experimentally by impedance and polarization measurements. Impedance spectroscopy can be used to clarify the processes occurring in a DMFC as well as to select the appropriate materials and different operating conditions such as working potential, methanol concentration, electrode structure, oxidant, etc. From these analysis, it is derived that a proper tailoring of the electrode structure is important for passive mode operation. However, the main problem is associated with methanol crossover; thus, it is mandatory to develop methanol impermeable membranes.

5.6. References

1. W. Qian, D. P. Wilkinson, J. Shen, H. Wang, J. Zhang, J. Power Sources 2006, 154, 202.

2. A. S. Aricò, S. Srinivasan, V. Antonucci, Fuel Cells 2001, 1, 133.

3. L. Carrette, K. A. Friedrich, U. Stimming, Chem. Phys. Chem. 2000, 1, 163.

4. A. Heinzel, C. Hebling, M. Muller, M. Zedda, C. Muller, J. Power Sources 2002, 105, 250.

5. H. Yang, T. S. Zhao, Q. Ye, J. Power Sources 2005, 139, 79.

6. G. Q. Lu, C. Y. Wang, J. Power Sources 2004, 134, 33.

7. D. Kim, E. A. Cho, S.-A. Hong, I.-H. Oh, H. Y. Ha, J. Power Sources 2004, 130, 172.

8. T. Ito, K. Kimura, M. Kunimatsu, Electrochem. Commun. 2006, 8, 973.

9. A. Blum, T. Duvdevani, M. Philosoph, N. Rudoy, E. Peled, J. Power Sources 2003, 117, 22.

10. S. C. Kelley, G. A. Deluga, W. H. Smyrl, Electrochem. Solid State Lett. 2000, 3, 407.

11. G. Jewett, Z. Guo, A. Faghri, J. Power Sources 2007, 168, 434.

12. Z. Guo, A. Faghri, J. Power Sources 2006, 160, 1183.

13. R. Chen, T. S. Zhao, J. Power Sources 2007, 167, 455.

14. R. Chen, T. S. Zhao, Electrochim. Acta 2007, 52, 4317.

15. R. Chen, T. S. Zhao, Electrochem. Commun. 2007, 9, 718.

16. M. A. Abdelkareem, N. Nakagawa, J. Power Sources 2007, 165, 685.

17. G. Q. Lu, C. Y. Wang, T. J. Yen, X. Zhang, Electrochim. Acta 2004, 49, 821.

18. G. D'Arrigo, C. Spinella, G. Arena, S. Lorenti, Fuel Cells Bull. 2003, 4, 10.

19. J. Bostaph, R. Koripella, A. Fisher, D. Zindel, J. Hallmark, in: Proceedings of the 199th Meeting on Direct Methanol Fuel Cells, Electrochemical Society, Washington D. C., USA, 25-29 March 2001.

20. J. Pavio, J. Hallmark, J. Bostaph, A. Fisher, B. Mylan, C.G. Xie, Fuel Cells Bull. 2002, 43, 8.

21. S. Motokawa, M. Mohamedi, T. Momma, S. Shoji, T. Osaka, Electrochem. Commun. 2004, 6, 562.

22. N. Sabate, J. P. Esquivel, J. Santander, N. Torres, I. Gracia, P. Ivanov, L. Fonseca, E. Figueras, C. Canè, J. New Mater. Electrochem. Sys. 2008, 11, 143.

23. S. W. Lim, S. W. Kim, H. J. Kim, J. E. Ahn, H. S. Han, Y. G. Shul, J. Power Sources 2006, 161, 27.

24. J. J. Martin, W. Qian, H. Wang, V. Neburchilov, J. Zhang, D. P. Wilkinson, Z. Chang, J. Power Sources 2007, 164, 287.

25. A. Lam, D. P. Wilkinson, J. Zhang, Electrochim. Acta 2008, 53, 6890.

26. Q. Mao, G. Sun, S. Wang, H. Sun, G. Wang, Y. Gao, A. Ye, Y. Tian, Q. Xin, Electrochim. Acta 2007, 52, 6763.

27. T. Frey, K. A. Friedrich, L. Jorissen, J. Garche, J. Electrochem. Soc. 2005, 152, A545.

28. X. Ren, M. S. Wilson, S. Gottesfeld, J. Electrochem. Soc. 1996, 143, L12.

29. A. K. Shukla, P. A. Christensen, A. J. Dickinson, A. Hamnett, J. Power Sources 1998, 76, 54.

30. A. S. Aricò, A. K. Shukla, K. M. el-Khatib, P. Cretì, V. Antonucci, J. Appl. Electrochem. 1999, 29, 671.

31. A. Oedegaard, C. Hebling, A. Schmitz, S. Moller-Holst, R. Tunold, J. Power Sources 2004, 127, 187.

32. Z.-G. Shao, F. Zhu, W.-F. Lin, P. A. Christensen, H. Zhang and B. Yi, J. Electrochem. Soc. 2006, 153, A1575.

33. V. Baglio, A. Stassi, F. V. Matera, V. Antonucci, A. S. Aricò, Electrochim. Acta 2009, 54, 2004.

34. A. Di Blasi, V. Baglio, T. Denaro, V. Antonucci, A. S. Aricò, J. New Mater. Electrochem. Sys. 2008, 11, 165.

35. J. G. Liu, T. S. Zhao, R. Chen, C. W. Wong, Electrochem. Commun. 2005, 7, 288.

36. B. K. Kho, B. Bae, M. A. Scibioh, J. Lee, H. Y. Ha, J. Power Sources 2005, 142, 50.

37. V. Baglio, A. Stassi, F. V. Matera, A. Di Blasi, V. Antonucci, A. S. Aricò, J. Power Sources 2008, 180, 797.

38. A. S. Aricò, V. Baglio, V. Antonucci, I. Nicotera, C. Oliviero, L. Coppola, P. L. Antonucci, J. Membr. Sci. 2006, 270, 221.

39. A. Oedegaard, J. Power Sources 2006, 157, 244.

40. S. Uhm, S. T. Chung, J. Lee, J. Power Sources 2008, 178, 34.

41. U. Krewer, M. Christov, T. Vidakovic', K. Sundmacher, J. Electroanal. Chem. 2006, 589, 148.

42. A. S. Aricò, V. Alderucci, V. Antonucci, S. Ferrara, V. Recupero, N. Giordano, K. Kinoshita, Electrochim. Acta 1992, 37, 523.

43. . Epelboin, C. Gabrielli, M. Keddam, in Comprehensive Treatise of Electrochemistry, vol. 9 (Eds. E. Yeager, J. O'M. Bockris, B. E. Conway and S. Sarangapani), Plenum Press, New York, 1984, 83.

44. D. Schumann, J. Electroanal. Chem. 1968, 17, 45.

45. R. D. Armstrong, M. F. Bell, A. A. Metcalfe, Electrochemistry 1978, 6, 98.

6. Performance and Application assessment

The stack has been designed to power a portable handheld device which specification are addressed in Table 6.1. The performances obtained from the planar system designed, operating in passive mode under ambient conditions, have been discussed in Chapter 3 and are reassumed in Table 6.2. By Assuming the figures shown in Tables 61. and 6.2 it is possible to envisage the general specifications of the final system as presented in Table 6.3.

Table 6.1.: application specifications

Maximum power	4,8 W
Nominal rated voltage	4,8 V
Nominal rated current	1 A

Table 6.2. Designed system specifications and best performance under passive operation in ambient conditions.

Catalyst	1:1 Pt/Ru
Catalyst Loading	4 mg/cm^2 (Pt) on both anode and cathode
Fuel concentration	5 M
Maximum specific power	20 mW/cm^2 @ 0,2 V/cell
OCV Voltage at peak power Current at peak power	0,6 V/cell 0,2 V/cell 100 mA/cm^2
Cell active area Cell active dimensions	4 cm^2 20 x 20 mm
Number of cells	3 in series-connected

Table 6.3. Complete system design specification as calculated from Table 6.1 and Table 6.2 data.

Single cell active area Single cell dimensions	6 cm^2 30 x 20 mm
Number of cells in a planar stack Number of cell arrays	24 cells (6 x 4) 2 arrays connected in series
Tank configuration	Double-face

6.1. Stack design

Fuel crossover is a major issue in terms of performance loss (smaller OCV), efficient fuel utilization and optimal system design. High methanol concentration increase significantly these problems, meanwhile a more concentrated fuel would reduce tank size (by reducing the amount of water which doesn't produce energy) or increase the autonomy by increasing the fuel amount in the same tank Hence crossover is a crucial issue which cannot be ignored. If the use a different polymer is excluded, some of the simplest ways to decrease fuel crossover is the use of thicker membrane. This would eventually increase the membrane ionic resistance and hence resulting in worse performances as well. Electrode structure can also be optimized, by managing its hydrophobic properties, to ease or impede water transport within the electrode and at the membrane-electrode interface.

Actual results have shown that the stack design, apart from MEA properties, can be an acceptable candidate for a portable system operating under ambient passive mode. Thus it can be considered validated and most of the future work should be addressed in increase the MEA, and especially the membrane, properties.

6.2. System design

A single three cell stack can not power a practical application as its maximum power is too low (Table 6.1). Hence its necessary to increase the maximum power by designing a larger stack, with a larger number of cells. This objective can be achieved in different ways: by designing a stack with a bigger number of cell of a larger active area or by assembling a number of smaller stacks properly designed and connected. As current requirement are achieved by dimensioning the single cell active area, and the rated voltage by increasing the number of cells connected in series, this process would lead to a large stack with a large number of cell. Moreover, its dimensions would easily result impractical in most portable application as it would result in a large area flat shaped stack.

A different approach is to design a stack by dimensioning either the number of cell to reach the required voltage (voltage design) or by dimensioning the active cell area to reach the required current (current design). In the first case, a sufficient number of such stacks will be connected in parallel to reach the required current. In the latter case, a sufficient number of such stacks would be connected in series to reach the required voltage. Both of these paths are acceptable and the choice depends mostly on the application required voltage and current. ON a practical side, it is important to design the single array to increase its output voltage as much as convenient. This is due to power electronics efficiency when used to decrease voltage.

When such devices are used to increase the voltage to match that of the application, it may result in impractical and unacceptable low efficiency. Hence it is very important to design the stack and the arrays obtaining the higher voltage possible (which is proportional to the number of cells connected in series).

In any case, with actual performances, a scale-up of the system would be meaningless until crossover issues will be solved, either with a different membrane or a different electrode structure able to reduce meaningfully such issue.

6.3. Conclusions

The results, shown in the previous chapters, demonstrated that the design has been correctly engineered and most of the limitation are due to membrane crossover issues.

The PCB-like system and MEA are easy to produce in large number and be scaled up to reach design performance required by the final application. Still, a big effort in base research is needed for methanol fuel cells to reduce both crossover issues and catalyst loading, this latter resulting in a more expensive system. Unless a different, more performing, solution will be found for methanol fuel cells operating in passive mode, probably hydrogen systems will be still more attractive for most fuel cell applications as they are more performing, stable and less expensive.

In such a case, the PCB-like design is very flexible and can be easily adapted to hydrogen systems as well with significant changes to tank, sealing and hopefully (and likely) with better performance.